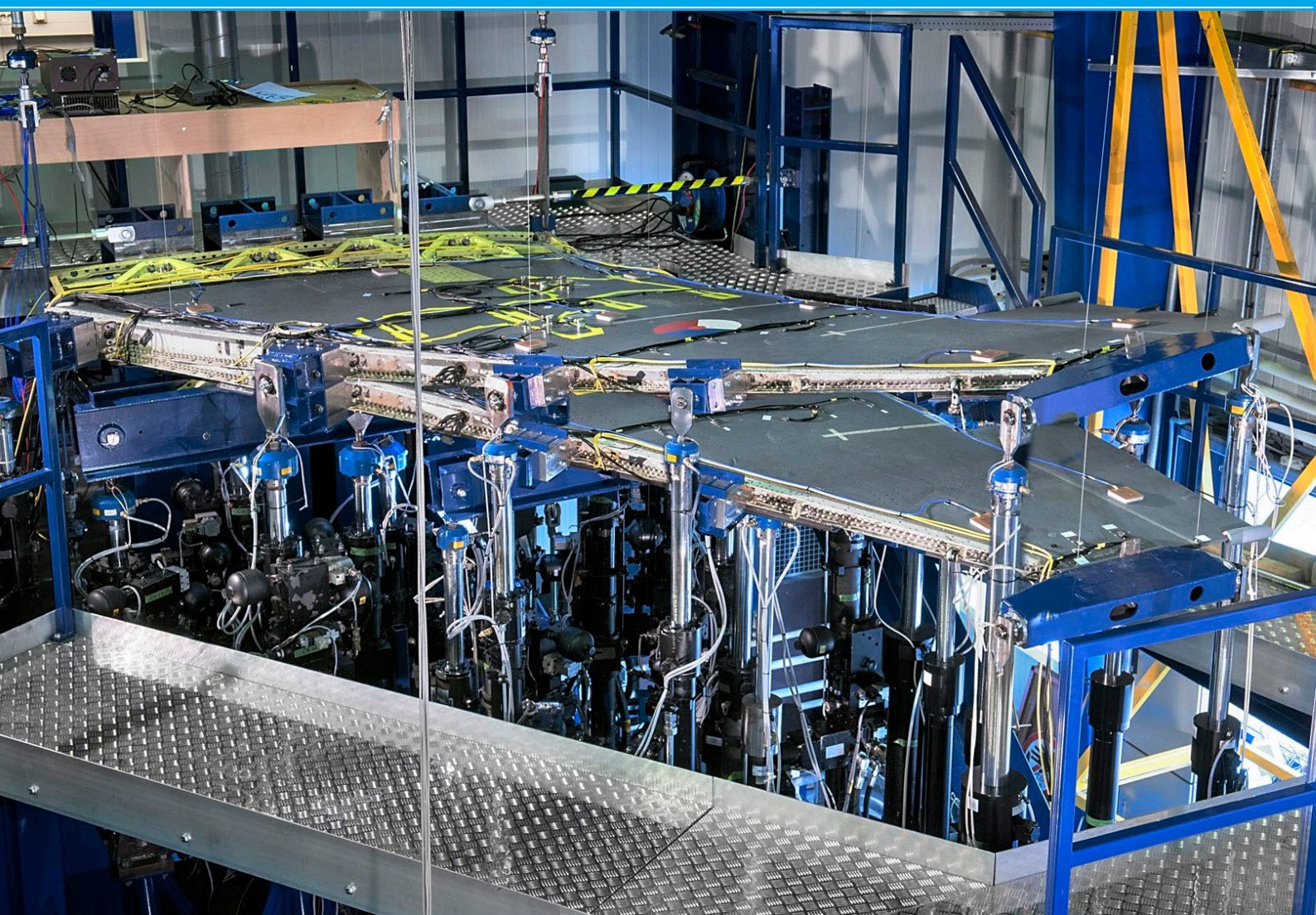




Review of aeronautical fatigue investigations in the Netherlands during the period March 2013 - March 2015

National Aerospace Laboratory NLR

NLR-TP-2015-123 – April 2015



NLR – Dedicated to innovation in aerospace

National Aerospace Laboratory NLR

Anthony Fokkerweg 2

1059 CM Amsterdam

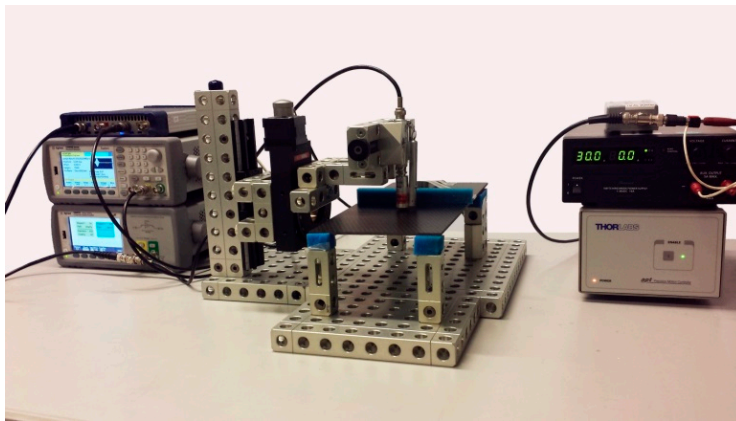
The Netherlands

Tel +31 (0)88 511 3113

www.nlr.nl

EXECUTIVE SUMMARY

Review of aeronautical fatigue investigations in the Netherlands during the period March 2013 - March 2015



Experimental setup for air-coupled ultrasound, used for structural health monitoring.

Description of work

This report is a review of the aerospace fatigue activities in the Netherlands during the period March 2013 to March 2015. The review is the Netherlands National Delegate's contribution to the 34th Conference of the International Committee on Aeronautical Fatigue and Structural Integrity (ICAF), 1 and 2 June 2015, Helsinki, Finland.

Report no.

NLR-TP-2015-123

Author(s)

M.J. Bos
G.M.H.J. Habets

Report classification

UNCLASSIFIED

Date

April 2015

Knowledge area(s)

Aircraft sustainment
Aircraft materials
Testing of aircraft structures and materials

Descriptor(s)

ICAF
Structural Fatigue
Structural Integrity
Damage Tolerance



Review of aeronautical fatigue investigations in the Netherlands during the period March 2013 - March 2015

M.J. Bos and G.M.H.J. Habets

Customer

National Aerospace Laboratory NLR

April 2015

Review of aeronautical fatigue investigations in the Netherlands during the period
March 2013 - March 2015

This report is based on a presentation held at the 34th Conference of the International Committee on Aeronautical Fatigue and Structural Integrity (ICAF), Helsinki, Finland, 1 and 2 June 2015.

The contents of this report may be cited on condition that full credit is given to NLR and the authors.

Customer National Aerospace Laboratory NLR
Contract number -----
Owner National Aerospace Laboratory NLR
Division NLR Aerospace Vehicles
Distribution Unlimited
Classification of title Unclassified
Date April 2015

Approved by:

Author M.J. Bos	Reviewer G.M.H.J. Habets	Managing department H.G.S.J. Thuis
Date 16/4/2015	Date 16/4/2015	Date 16-4-2015



Summary

This report is a review of the aeronautical fatigue activities in the Netherlands during the period March 2013 to March 2015, and is the National Delegate's contribution to the 34th Conference of the International Committee on Aeronautical Fatigue and Structural Integrity (ICAF), 1 and 2 June 2015, Helsinki, Finland.

This page is intentionally left blank.

Contents

Abbreviations	7
1 Introduction	9
2 Structural Load/Usage/Health Monitoring	9
2.1 Sensors for monitoring corrosivity in NH90 helicopters	9
2.2 RNLAf C-130H(-30) fatigue loads & usage monitoring	11
2.3 RNLAf F-16 Block 15 fatigue loads & usage monitoring	11
2.4 Fatigue loads & usage monitoring of the RNLAf helicopter fleets	12
2.5 Multi-nation NH90 Supportability Data Exchange programme	14
2.6 FBG sensor network design for detection of skin-stringer debonds in fuselage panels	16
2.7 Evaluation of three different Structural Health Monitoring technologies	18
2.8 Vibration based Structural Health Monitoring of Composite Skin-stiffener Structures	20
3 Fibre/Metal Laminates/Structures	21
3.1 Methodology for analysis of MSD in Fibre Metal Laminates	21
3.2 Directionality of Damage Growth in Fibre Metal Laminates	22
3.3 Lay-up Optimisation of Fibre Metal Laminates	24
4 Composite Materials & Structures	25
4.1 Fatigue Behaviour of Impact Damaged Thick-Walled Composites	25
4.2 Physics based methodology for describing interlaminar ply delamination growth under mode I	28
4.3 Towards fundamental understanding on interlaminar ply delamination growth under mode II and mixed-mode	30
5 Adhesively Bonded Structures.....	33
5.1 Characterising the energy balance for fatigue crack growth in adhesive bonds	33
5.2 Mixed-mode fatigue disbond on metallic bonded joints	34
5.3 Effects of Variable Amplitude Fatigue and Temperature on the Durability of Composite Bonded Repairs	35
6 Metallic Materials and Structures	36
6.1 Development of Physics-based principles of similitude	36

Review of aeronautical fatigue investigations in the Netherlands during the period
March 2013 - March 2015

6.2	Improved life assessment for complex geometries	37
6.3	NASGRO stress intensity solution development for a displacement controlled corner crack	40
6.4	F-16 Wing crack severity index evaluation	41
6.5	F-16 wing test lead crack growth analyses	43
6.6	Fatigue crack growth characterization of 3D printed Ti-6Al-4V	44
6.7	The influence of stress state on the fatigue crack growth rate power law exponent	46
7	Non-Destructive Evaluation.....	47
7.1	Air-Coupled Ultrasound	47
7.2	Detection of barely-visible impact damage in composite plates using Lamb waves	48
7.3	Optical coherence tomography for material characterization	50
7.4	Structural Health Monitoring based on Time_Reversal Lamb Waves	51
8	Full-scale Testing.....	52
8.1	F-16 Block 15 Wing Damage Enhancement Test	52
9	Special Category.....	55
9.1	Milestone Case Histories in Aircraft Structural Integrity (Update 2015)	55
10	References.....	56

Abbreviations

Acronym	Description
A	Asymmetric
AE	Acoustic Emission
ACT	Air-Coupled ultrasound Transducer
AIM	Aircraft Integrity Management
ASME	American Society of Mechanical Engineers
ATRI	Aero Technology Research Institute (of the Republic of Korea Air Force)
BVID	Barely Visible Impact Damage
CAD	Computer-Aided Design
CCP	Central Cut Ply
CFRP	Carbon Fibre Reinforced Polymer
CHAMP	CHinook Airframe Monitoring Programme
CPU	Central Processor Unit
CSI	Crack Severity Index
CVFDR	Cockpit Voice and Flight Data Recorder
CVM	Comparative Vacuum Monitoring
DADTA	Durability and Damage Tolerance Analysis
DCB	Double Cantilever Beam
DCPD	Direct Current Potential Drop
DIC	Digital Image Correlation
DSTO	Defence Science and Technology Organisation
F&DT	Fatigue and Damage Tolerance
FBG	Fibre Bragg Grating
FEM	Finite Element Method
FML	Fibre/Metal Laminate
FRP	Fibre Reinforced Polymer
G	Strain Energy Release Rate
GLIMS	Ground Logistics Information Management System
ICAF	International Committee on Aeronautical Fatigue and Structural Integrity
HIP	Hot Isostatic Pressing
LEFM	Linear Elastic Fracture Mechanics
LH	Left Hand
LHS	Left-Hand Side
LM	Lockheed Martin
LOV	Limit of Validity
MDS	Monitoring and Diagnostics System
MSD	Multiple-site Damage
MSE-DI	Modal Strain Energy Damage Index
MTBF	Mean Time Between Failure
NAHEMA	NATO Helicopter Management Agency

Review of aeronautical fatigue investigations in the Netherlands during the period
March 2013 - March 2015

NATO	North Atlantic Treaty Organization
NDE	Non-Destructive Evaluation
NDT	Non-Destructive Testing
NFH	NATO Frigate Helicopter
NLR	National Aerospace Laboratory NLR (of the Netherlands)
OCE	Optical Coherence Elastography
OCT	Optical Coherence Tomography
PZT	Piezoelectric Transducer
R	Stress ratio
R&D	Research and Development
RH	Right Hand
RNLAF	Royal Netherlands Air Force
RR	Rotorrounds
S	Symmetric
SARISTU	Smart Intelligent Aircraft Structures
SDE	Supportability Data Exchange
SERR	Strain Energy Release Rate
SIF	Stress Intensity Factor
SIPS	Structural Integrity of Pressurised Structures
SHM	Structural Health Monitoring
SLM	Selective Laser Melting
STF	Strain Transfer Factor
TRLW	Time Reversal of Lamb Waves
TTH	Tactical Transport Helicopter
TUD	Technical University of Delft
USV	Ultrasonic Verification
UT	University of Twente
WAF	Wing Attachment Fitting
XFEM	Extended Finite Element Method

1 Introduction

The present review gives a summary of the work performed in the Netherlands in the field of aerospace fatigue during the period from March 2013 to March 2015. The contributions to this review come from the following sources:

- The National Aerospace Laboratory (NLR)
- The Faculty of Aerospace Engineering, Structural Integrity & Composites, Aerospace Non-Destructive Testing Laboratory, Delft University of Technology (TUD)
- The Faculty of Engineering Technology, Chair of Production Technology, University of Twente (UT)
- Amsterdam University of Applied Sciences (HvA)

The names of the principal investigators and their affiliations are given at the start of each topic. The format and arrangement of this review is similar to that of previous years.

2 Structural Load/Usage/Health Monitoring

2.1 Sensors for monitoring corrosivity in NH90 helicopters

Principal investigator(s): L. 't Hoen-Velterop, NLR

The NH90 helicopter has two main variants; the TTH is designed as transport helicopter, while the NFH is designed for operations above sea, either from an airbase close to the coast or from a ship. The current maintenance manuals call for a severe maintenance burden when operating in saline environment, especially for ship-based operations. However, they do not differentiate in geographical location of the operations.

The first years of in-service experience have shown that corrosion on the helicopters is much more severe when the helicopter has operated from a ship in tropical areas than when the helicopter has operated in more moderate climates. Monitoring of the environment with corrosion sensors will allow for condition based corrosion inspections and maintenance and prevent over-maintenance. The corrosion sensors selected for this purpose measure the following parameters that indicate the corrosiveness of the environment:

- Air temperature
- Surface temperature
- Relative humidity
- Time of wetness / fluid conductivity
- Corrosion rate of a AA7075-T6 probe

Review of aeronautical fatigue investigations in the Netherlands during the period
March 2013 - March 2015

The sensors are placed on the upper deck of the helicopter and in the cabin. As a reference two of the same sensors are placed on the ship; one in the hangar and one outside near the helicopter deck. The sensors on the ship are accompanied by 6 galvanic corrosion coupons with material combinations representative for the NH90 helicopter.

The first results show that the helicopter experiences conditions that are more severe than in the hangar, but less severe than on the helicopter deck (Figure 1). The corrosion coupons indicate very severe conditions on the helicopter deck (Figure 2), which is confirmed by the sensor measurements.

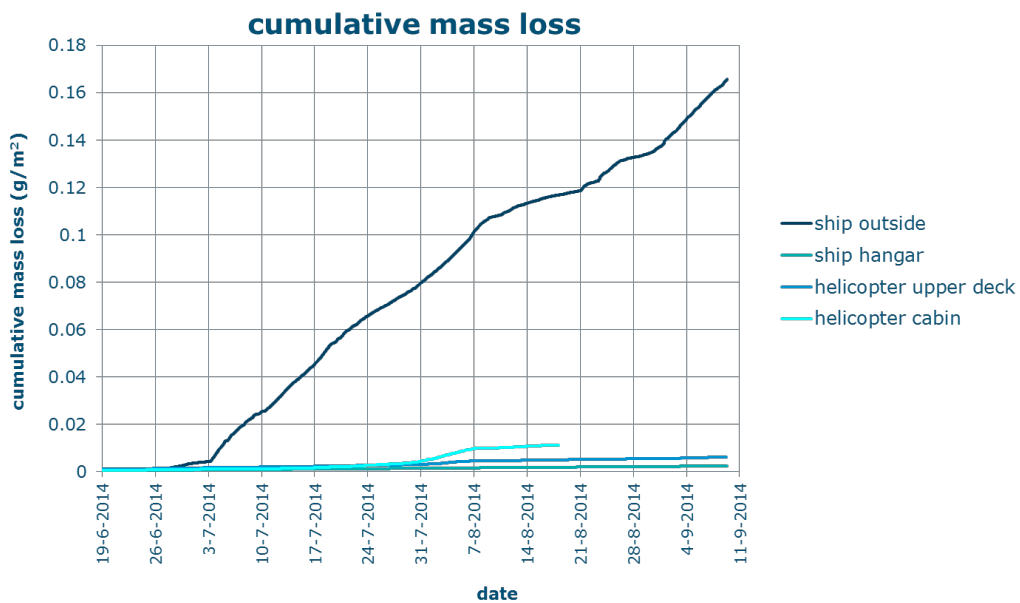


Figure 1: Cumulative mass loss results after 3 month exposure on a ship, measured with a AA7075-T6 corrosion rate probe.

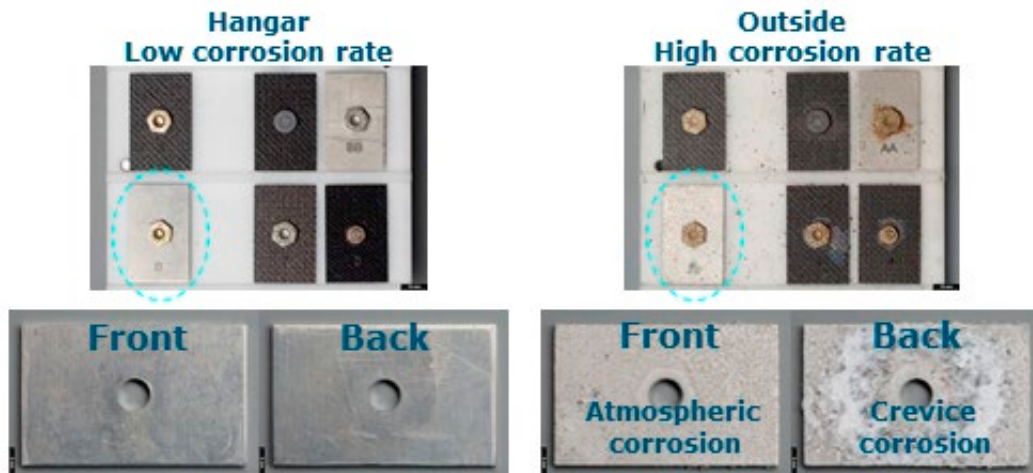


Figure 2: Corrosion coupons after 3 month exposure on a ship.

2.2 RNLAf C-130H(-30) fatigue loads & usage monitoring

Principal investigator(s): M.J. Bos and J.A.J.A. Dominicus, NLR

The Royal Netherlands Air Force (RNLAf) operates a mixed fleet of C-130H and C-130H-30 (stretched fuselage) models. In 2001 the NLR has been tasked to monitor the usage of the fleet and to routinely keep track of the consumed fatigue life of the major airframe components of each of the individual aircraft in the fleet. For this purpose NLR has developed an individual aircraft monitoring programme dubbed “HOLMES”. This programme is based on the collection of operational data from various sources, including a flight data recorder, and the subsequent translation of these data to the accrued structural fatigue damage at twelve control points in the airframe. In addition the so-called severity factor per flight is calculated, which can be used to compute the Equivalent Flight Hours (EFH) that form the basis for fleet life management.

This on-going programme has already been described in the previous national review [1] and in a dedicated paper [2]. New is the joint development of a damage tolerance based programme (as compared to the current safe life approach) with the Aero Technology Research Institute (ATRI) of the Republic of Korea Air Force. For this purpose, ATRI is currently installing a flight test instrumentation system in a C-130H of the Republic of Korea Air Force.

2.3 RNLAf F-16 Block 15 fatigue loads & usage monitoring

Principal investigator(s): F.C. te Winkel, NLR

Structural fatigue loads & usage monitoring of the RNLAf/F-16 Block 15 fleet has been done routinely by the NLR since 1990. During the 1990s a new fatigue monitoring system specified by the NLR was developed by RADA by extending their ACE pilot debriefing system with loads and usage monitoring functionality: FACE (Fatigue Analysis & Air Combat Evaluation system). The main features of FACE are (a) an increase to five strain gauge locations, two indicative for wing root and “outer” wing bending, two at the rear fuselage dealing with horizontal and vertical tail loads and one in the fuselage centre section indicative for fuselage bending; (b) a flexible selection of flight, engine, and avionics parameters available via the MUX-BUS; and (c) fleet-wide implementation (since 2003) allowing more extensive load monitoring of each individual aircraft and systems.

The programme has already been reported in previous national reviews – see for instance ref. [1]. Recently added capabilities are:

- F-16 dynamic effects including limit cycle oscillation (LCO) tracking capability
- Landing Gear Damage Indicator
- Damage index for canopy pressure related ASIP control points

Proven benefits of the programme are:

- Valuable instrumentation package for Force Management purposes as part of the Aircraft and Engine Structural Integrity Programs ASIP and ENSIP
- Generation of test sequences based on actual measurements, for the F-16 Wing Damage Enhancement Test (see section 8.1)
- System has been a valuable source for mishap investigation
- Very flexible instrumentation package (each aircraft in theory a “unique” test aircraft)
- In recent years more ad hoc recordings have been made to support several research programmes:
 - Detailed engine FAULT-code recordings
 - Flight departure margin study
 - MFOQA (Military Flight Operations Quality Assurance) trial 2007 and 2011 with 18 aircraft instrumented with a dedicated measurement configuration
- Information system is frequently used as a study for development of next generation decision support and simulation tools

2.4 Fatigue loads & usage monitoring of the RNLAf helicopter fleets

Principal investigator(s): A. Oldersma, P. Vos, NLR

The Royal Netherlands Air Force (RNLAf) has tasked the National Aerospace Laboratory NLR with developing an airframe loads & usage monitoring programme for their CH-47D transport helicopter fleet. After an initial pilot phase during which the technical and operational possibilities were explored, a routine programme named “CHAMP” (CHinook Airframe Monitoring Programme) was started in 2007. In addition to a fleet wide installation of a Cockpit Voice & Flight Data Recorder (CVFDR) for the collection of the relevant parameters from the digital avionics data bus, two D-model Chinook airframes have been equipped with a state-of-the-art data acquisition system and nine strain gauges each, which are recorded at a high sample rate. In 2014 a third F-model Chinook was instrumented. All data processing is performed off-board; no on-board data reduction is done. This has led to an extensive and ever-growing database that can be used to conduct analyses that go beyond those traditionally performed within a loads & usage monitoring programme.

The recorded flight parameters serve as the input for Flight Regime Recognition. For validation purposes and to improve the Flight Regime Recognition algorithms, well-documented test flights were used to compare defined and pilot flown manoeuvres with the Flight Regime Recognition results. These scripted flights were also used to study the severity of manoeuvres. Therefore fatigue calculations were performed on flight segments. Two segment (window) sizes were selected, i.e. one rotor round (RR) window and a 15 rotor rounds (4 seconds) window. Although the relative fatigue damage per window is indicative only and the summation will not be the same as the calculated damage on a flight-by-flight basis, comparison with damage values per

whole flight shows that the differences are small. Figure 3 shows the ‘window’ fatigue damage for LH and RH turning manoeuvres.

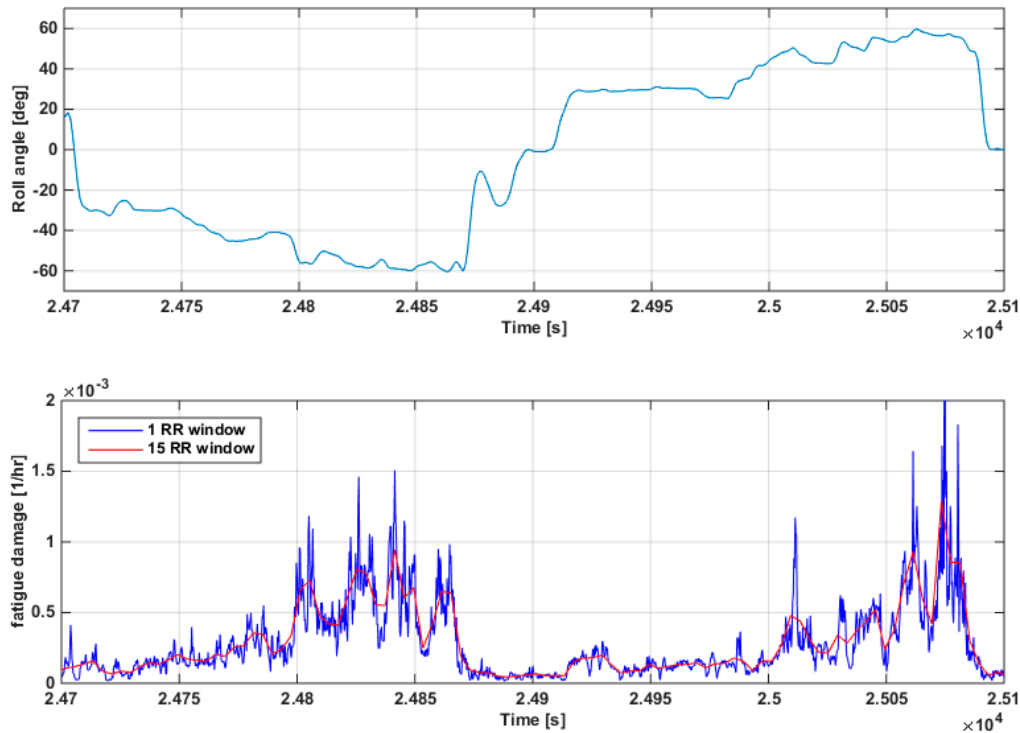


Figure 3: Severity of turning manoeuvres at different roll angles.

The Flight Regime distribution, together with other usage statistics such as weight distribution classes and speed classes, reveals differences in usage during out-of-area operations and usage within the Netherlands. The usage statistics are also used to serve as input for Usage Based Maintenance efforts. Knowing the actual usage, a more accurate estimate can be made of component retirement times. However, using the actual usage the level of reliability will be reduced because of the conservatism inherent to the design usage spectrum (based on worst case usage). Additional component retirement life reduction factors must be used to maintain a desired level of reliability.

Part of this work has already been reported in the previous national review [1] and in a dedicated paper [3]. New is the shifting focus from the airframe to the dynamic helicopter components. The objective is to enable the transition from calendar based maintenance to condition based maintenance for these components. As demonstrator components the forward and aft synchronizing shaft assemblies are being considered. It has been shown that the OEM specified retirement lives are very conservative and that life extension is possible based on monitoring of the actual usage. The process to accomplish this in a certified manner is currently being developed. Some details are provided in ref. [4].

Prompted by the success of the Chinook usage monitoring programme, the RNLAf has tasked NLR to develop similar programmes for the Apache AH-64D and NH90 helicopters. For this purpose Automatic Flight Regime Recognition algorithms have recently been developed for these helicopter types; they will form the backbone of the AH-64D and NH90 usage monitoring programmes which are currently being developed.

2.5 Multi-nation NH90 Supportability Data Exchange programme

Principal investigator(s): A.A. ten Have, NLR

Under contract of NAHEMA, NLR has developed and implemented a so-called NH90 Supportability Data Exchange (SDE) service for a consortium serving nine nations that operate the NH90/MRH90 helicopter. It consists of a common shared usage database and analysis toolbox with automated web based user data input.

The full NH90 SDE service comprises the following elements:

1. An Occurrence Reporting System functionality which provides all participating nations with a capability to store, analyze, report and share NH90 SDE occurrence data in a flexible, secure environment, allowing adequate communication of occurrence reports between military headquarters, operational fields and maintenance facilities.
2. A Reliability Assessment System functionality which provides the NH90 operator with the capability to determine experienced failure rates (MTBFs) of different helicopter components based on parts and equipment failures and maintenance task information. The SDE system contains provisions to extend reliability calculations towards Availability and Maintainability calculations, in the future.
3. An Aircraft Integrity Management functionality which offers a threefold state-of-the-art structural integrity and fleet life management tool with a standard reporting facility. Input data for SDE Level 3 AIM can be from different sources, e.g. MDS-GLIMS, Flight Data Recorder or a nation specific non-integrated retro-fit multi-channel data acquisition unit for strain gauge measurements, fed by data from the helicopter digital data buses.
4. A public and secure website (see: <https://sde.nlr.nl>), a moderated forum and a yearly users conference to evaluate and discuss integrity, completeness and validity of NH90 usage data, analysis results, helicopter degradation and maintenance, and to manage and direct necessary future SDE engineering support.

In 2012 the SDE Reliability Assessment System and the Occurrence Reporting System became fully functional. Physically, the NH90 SDE service is running on a 24/7 basis in a secure environment, located at NLR-Flevoland.

In the past years 2013-2015 the participating nations have started uploading their occurrences and event data for reliability calculations. In October 2014 the 2nd SDE user conference was held, hosted by the French Army, during which the first comparisons could be made between the 9 participating nations.

Figure 4 below illustrates the number of occurrences as of January 2014. In the meantime, this number has increased to approximately 2500 occurrences by January 2015. The sources of the respective occurrences is indicated in Figure 5, showing that most NH90 occurrences originate from issues, labeled General, Circumstances, Additional and Equipment. It has to be noted that these indications are rather premature, because most participating nations are still in the process of generating a Business-to-Business interface to achieve autonomous data upload into the SDE service at NLR in the Netherlands.

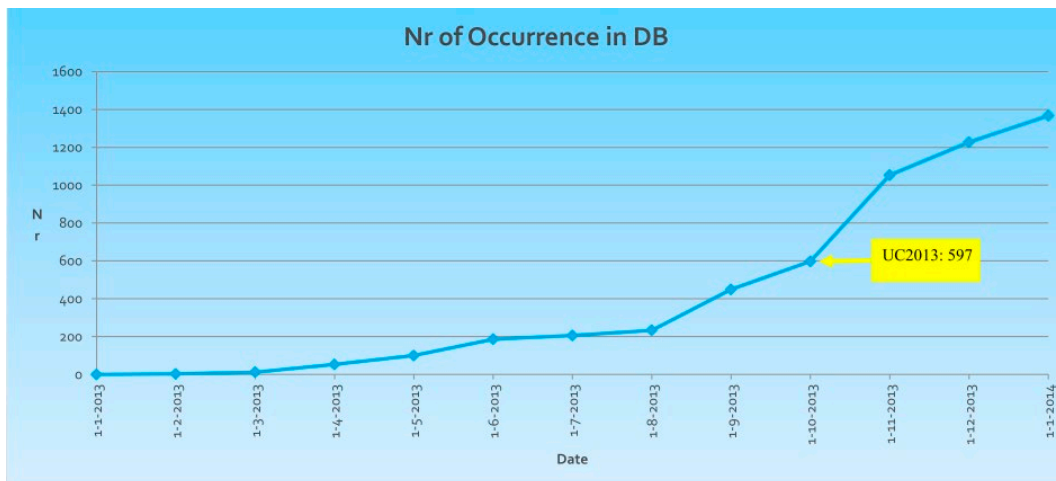


Figure 4: Number of NH90 occurrences in the database, status January 2014.

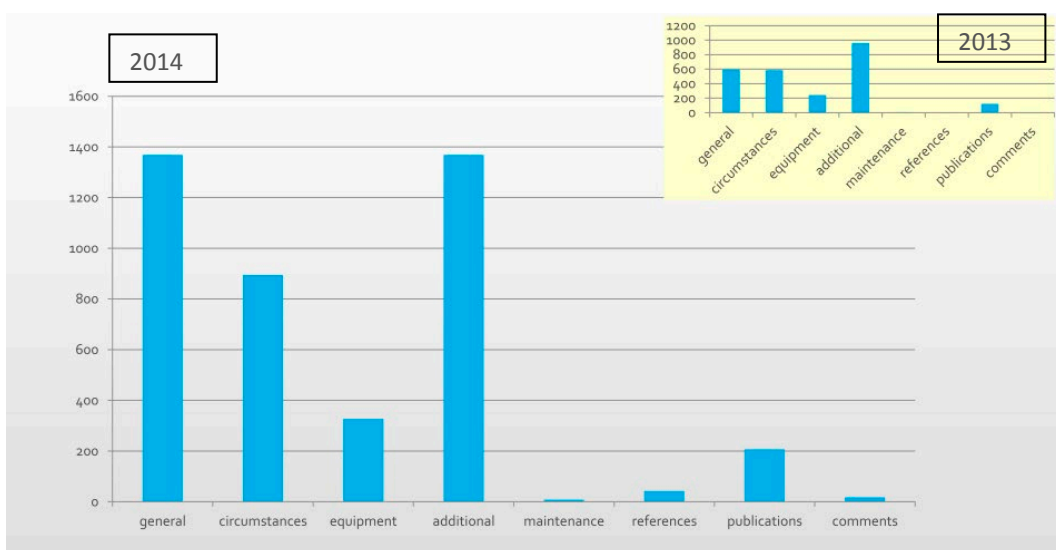


Figure 5: Sources of NH90 occurrences.

2.6 FBG sensor network design for detection of skin-stringer debonds in fuselage panels

Principal investigator(s): F.P. Grooteman, NLR

Within the European project SARISTU (Smart Intelligent Aircraft Structures) one of the objectives is to examine the capability of optical Fibre Bragg Grating (FBG) sensors to detect damage. This type of sensor offers a number of advantages for application in aircraft structures, such as light weight, tolerance for harsh environments, long term stability, complete passivity and no interference with other signals. The FBG sensor output correlates to the local strain. One of the promising algorithms for damage detection of skin-stringer debonds is damage indicators based on a modal approach where a previous state is compared with the current state.

Within SARISTU an existing structural health monitoring (SHM) system design tool has been extended (Figure 6). The design tool is highly automated and can be applied to examine a strain sensor network (number and location) for its suitability for damage detection. Embedding or surface mounting of sensors can be easily taken into account as well.

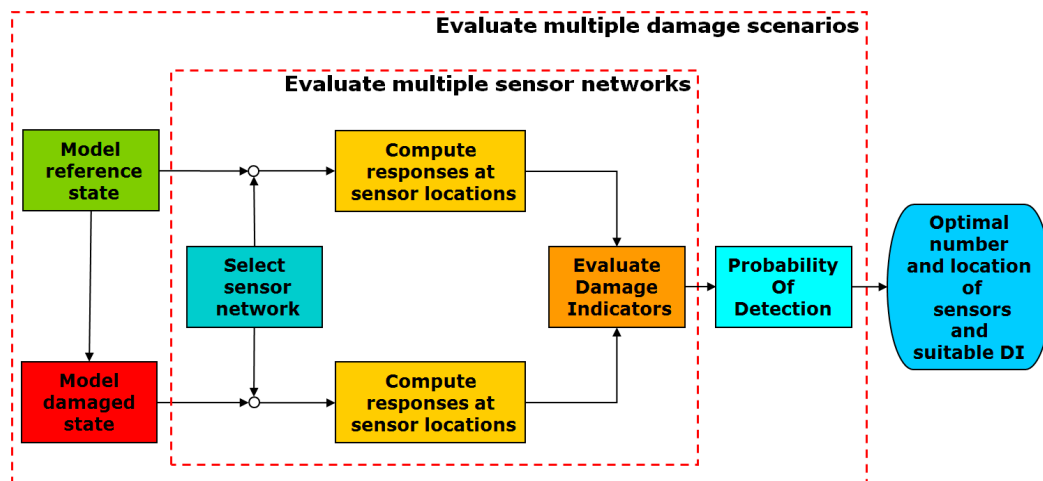


Figure 6: Flow diagram of the SHM damage detection design tool.

Within SARISTU various FBG sensor networks were examined for different (flat and curved) fuselage panels. An example is presented in Figure 7 and Figure 8, which show a composite skin with hat stiffeners and aluminium clips and frames.

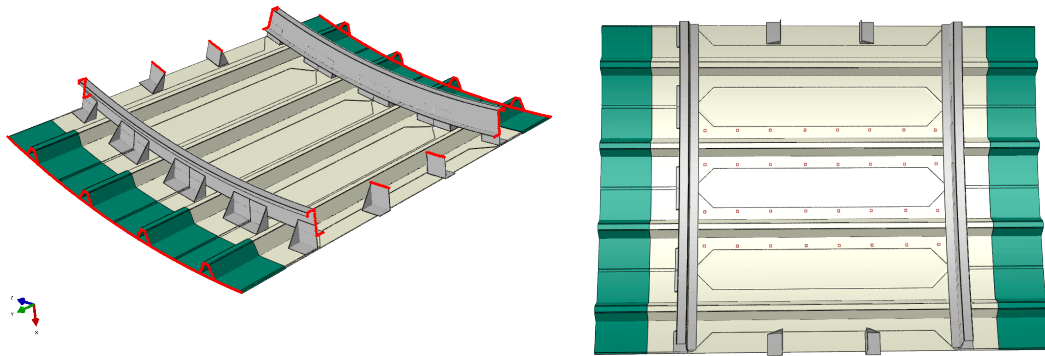


Figure 7: FBG sensor network design for a SARISTU fuselage panel.

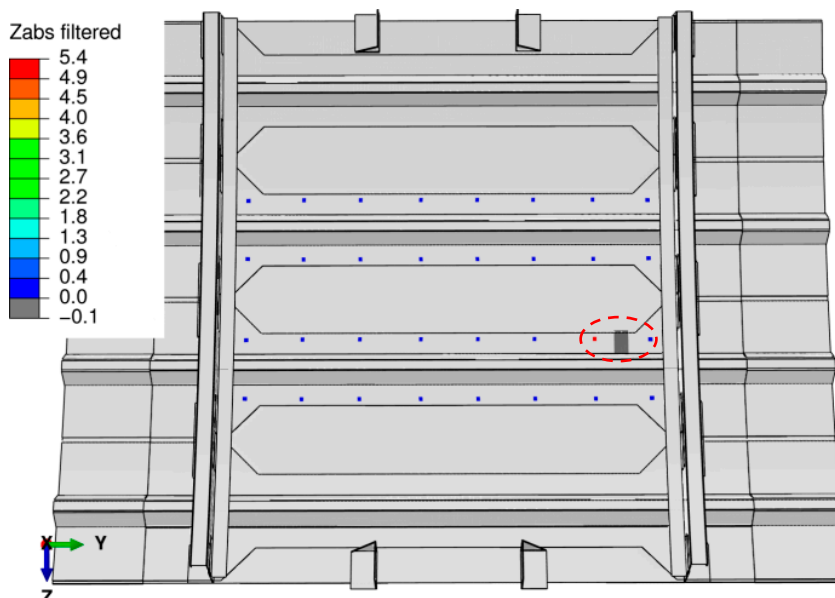


Figure 8: Damage indicator values signaling damage (in red), a simulated skin-stringer debond (in grey).

A final sensor network was determined to minimise the number of sensors to detect the presence and location of skin-stringer debonds of the two inner stringers. Even larger (20x20 mm²) impact damages in the middle bays should be detectable. A much more dense sensor network is required for the current damage indicators to be able to determine the size of the damage. This can be further improved by adding other damage indicators, requiring more advanced interrogators which are currently in development at the Dutch company Technobis Fibre Technologies.

An experimental program on two flat and two curved panels is planned within SARISTU to evaluate the capabilities of the FBG sensor networks for realistic airframe structures.

2.7 Evaluation of three different Structural Health Monitoring technologies

Principal investigator(s): J.H. Heida and J.S. Hwang, NLR

The left-hand side wing of a decommissioned F-16 Block 15 aircraft of the Royal Netherlands Air Force (RNLAf) was fatigue tested to more than two times the design life. Information about this test programme is provided in section 8.1 and in ref. [5].

In addition to the instrumentation with conventional strain gauges (e.g. single gauges, full bridges and rosettes) also special load monitoring and structural health monitoring (SHM) techniques were used during the test (Figure 9 and Figure 10). For load monitoring the data of conventional resistance strain gauges were compared with the response of optical fibre Bragg gratings (FBG). A total of 19 FBG's were installed on the upper wing skin, divided over three fibres. Two FBG interrogators were used: a Deminsys system of Technobis Fibre Technologies (wave length range 830 - 870 nm) and an IFIS100 system of the Korean company Fiberpro (wave length range 1510 - 1595 nm). For SHM the acoustic emission (AE) and comparative vacuum monitoring (CVM) techniques were employed to monitor fatigue crack initiation and growth. AE continuous monitoring was done with a 16-channel SAMOS AE system (Physical Acoustics B.V.) and 16 resonant sensors (150 kHz) covering five critical locations on the upper and lower wing skin. A CVM laboratory system (Structural Monitoring Systems) with nine S0400 intercept CVM sensors was used for fatigue crack detection at the 'finger' areas of the lower wing attachment fittings under periodic monitoring.

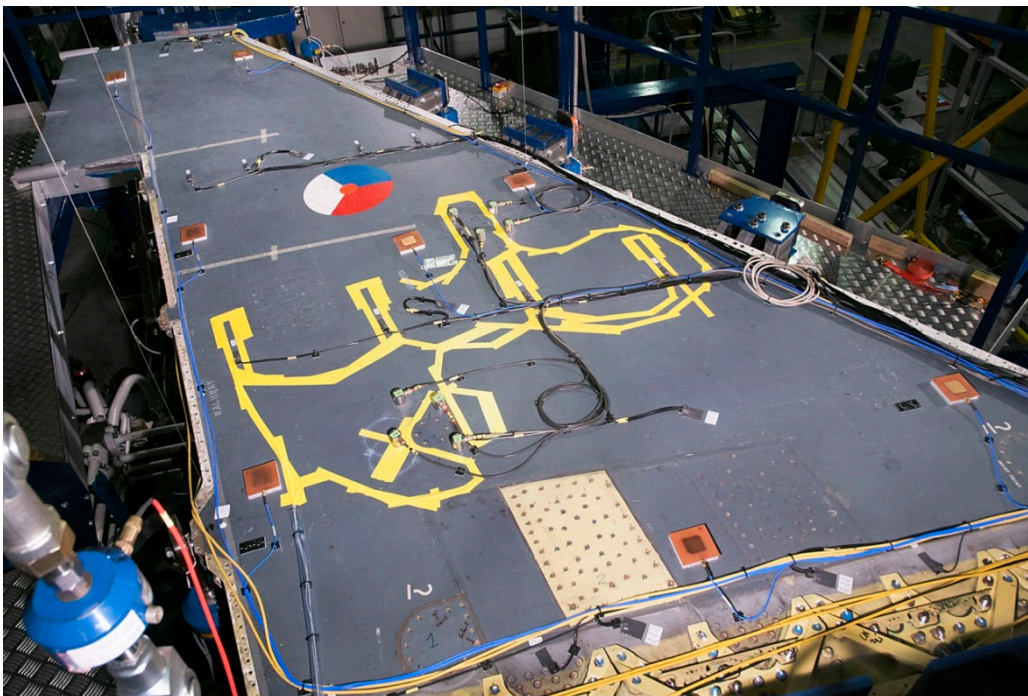


Figure 9: Monitoring of the F-16 LHS upper wing skin with AE and FBG sensors.

With the optical fibres a linear correlation between the FBG's and the conventional strain gauges was obtained using a specific strain transfer factor (STF). The average absolute error percentage was 1.3% and 97% of all FBG strain measurements were within $\pm 5\%$ of the strain gauge measurements. The SHM techniques, on the other hand, were less successful. For the CVM technique no crack indications were obtained during the test but, although fatigue cracks occurred in the fittings and in the bolt holes connecting the fittings to the wing skin, no cracks had in fact occurred at the locations under CVM monitoring. A positive result of the CVM measurements was that no false calls occurred during the complete test. Further, the AE system under continuous monitoring registered a lot of AE activity from different sources (also after drastic filtering of the AE data) but the AE data could not be reliably related to the initiation and growth of fatigue cracks in the areas monitored. Most of the AE activity was probably caused by mechanically induced noise such as frictional noise from the fastener locations and other surface rubbing areas (e.g. between skin and wing attachment fittings).

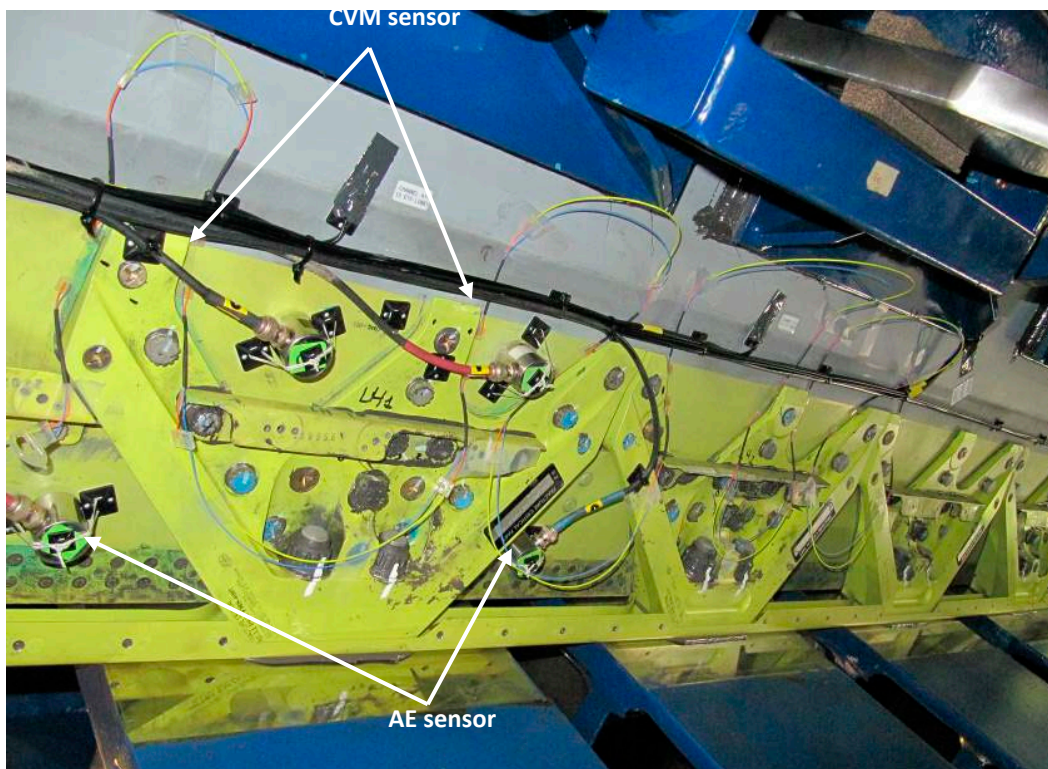


Figure 10: CVM and AE monitoring of the 'finger' areas of the WAF's on the lower wing skin.

2.8 Vibration based Structural Health Monitoring of Composite Skin-stiffener Structures

Principal investigator(s): T.H. Ooijevaar, UT

Composite materials combine a high strength and stiffness with a relatively low density. These materials can, however, exhibit complex types of damage, like transverse cracks and delaminations. These damage scenarios can severely influence the structural performance of a component. Periodic inspections are required to ensure the integrity of a component during its life. The current inspection methods are often time-consuming, costly and require the components to be readily accessible.

Vibration based structural health monitoring (SHM) technologies propose a promising alternative and involve the continuous monitoring of a structure by employing an integrated sensor system. These methods are based on the concept that the dynamic behavior of a structure can change if damage occurs. Although many damage identification methods have been proposed in the literature, there are still numerous difficulties in the practical application of these approaches, especially to complex structures. The performance of a vibration based damage identification approach is highly dependent on the actual design of the structure and the damage scenario that is considered.

This project focused on the identification of damage in advanced composite skin-stiffener structures. The principle objective was to develop guidelines for the detection, localization and characterization of damage in composite skin-stiffener structures based on changes in the dynamic behavior.

A literature study supported by an analytical model showed that mode shape curvatures combined with the modal strain energy damage index (MSE-DI) algorithm are a potentially powerful damage feature and classifier for the identification of damage in several advanced composite skin-stiffener structures. An experimental set-up, including a shaker and laser-vibrometer, was used to measure the dynamic responses. A linear dynamic system description is obtained by applying experimental modal analysis. The vibration experiments demonstrated the feasibility of the MSE-DI algorithm to detect, localize and roughly estimate the size of barely visible impact damage (BVID) in advanced composite skin-stiffener structures. It is concluded that the method is particularly effective for health monitoring of skin-stiffener connections. The method remained inconclusive in the case of pure skin related damage.

Experiments showed that damage at the skin-stiffener interface can introduce clear nonlinear effects in the dynamic behavior of the structure. These nonlinear effects are attributed to the interaction between the skin and stiffener that occurs during opening and closing motion of the damage. It is shown that linear damage identification methods (e.g. modal domain methods) are feasible for low excitation amplitudes, but the presence of nonlinear dynamic effects cannot remain silent for higher amplitudes. The nonlinear dynamic effects can act as strong indicator of

damage, but can also be useful for characterization purposes. The nonlinear dynamic effects introduced by the skin-stiffener damage urges the development of nonlinear damage identification methods. A study on the understanding and feasibility of using nonlinear vibro-acoustic modulations for the detection, localization and characterization of impact damage in a composite T-beam is presented. A time domain analysis at multiple spatial locations is used to detect and localize impact damage in a skin-stiffener connection, based on locally increased amplitude modulation effects. Analysis of the characteristics of the nonlinear modulations opens the ability to characterize the nonlinear dynamic behavior introduced by the damage at the skin-stiffener interface.

The work showed that the relations between the characteristics of the structure, the potential damage scenarios and the damage identification method together define the performance of the vibration based damage identification strategy. Therefore, it is concluded that the design of a vibration based damage identification strategy is made-to-measure work and requires a thorough physical understanding of the potential failure mechanisms, the critical damage locations and their effect on the dynamic behavior. To aid in this process, a scenario based procedure for the design of a damage identification strategy is proposed. All findings presented in this thesis contribute to the development of a design tool for research engineers, to assist the implementation of structural health monitoring technology in safety-critical composite structures.

The PhD dissertation is available from the UT library repository [6].

3 Fibre/Metal Laminates/Structures

3.1 Methodology for analysis of MSD in Fibre Metal Laminates

Principal investigator(s): W. Wang, C.D. Rans, R. Benedictus, TUD

The philosophy of damage tolerance assessment for fatigue crack growth in Fibre/Metal Laminates (FMLs) has been well established. These damage tolerance analyses for FMLs mainly focus on predicting the evolution of an isolated crack. As a result, they may be invalid due to the presence of Multiple-site Damage (MSD) cracks in fibre metal laminate structures. In order to combat the possibility of the failure caused by occurrence of MSD scenario, the airworthiness regulations has been revised in 2010 to include the definition of a Limit of Validity (LOV) placing limits on damage tolerance analyses.

In light of LOV, an analysis philosophy for predicting MSD crack growth in FMLs is proposed based on the approaches utilized in damage tolerance analyses for FMLs. Directly applying damage tolerance models to simultaneously predict the crack states of all MSD cracks in FMLs is cumbersome and computationally inefficient due to the complicated calculation of load

redistribution among multiple cracks and corresponding bridging fibres. Therefore the analysis philosophy is proposed to develop a simplified prediction methodology for analysing MSD behaviour in FMLs.

The interaction between cracks in FMLs can be idealized in terms of load redistribution. This concept of load redistribution in FMLs has been validated by investigating the effect of the presence of discretely notched layers on the crack growth in FMLs as the first step.

As can be seen in Figure 11, the crack growth rate of the crack with adjacent discretely notched Al layers is much higher than other two, especially when the crack gets close to the notch edge. This is attributed to the fact that notched Al layers lead to more stiffness reduction and more load redistributed from the location of notch to the crack tip in the FML panel.

Additionally, the growth behaviour of an eccentric crack with two different delamination shapes on both sides of its saw-cut in a FML panel is being studied. Integrating the analysis method for load redistribution mechanism and analysis model for eccentric crack in FMLs could lead to the simplified model for MSD analysis.

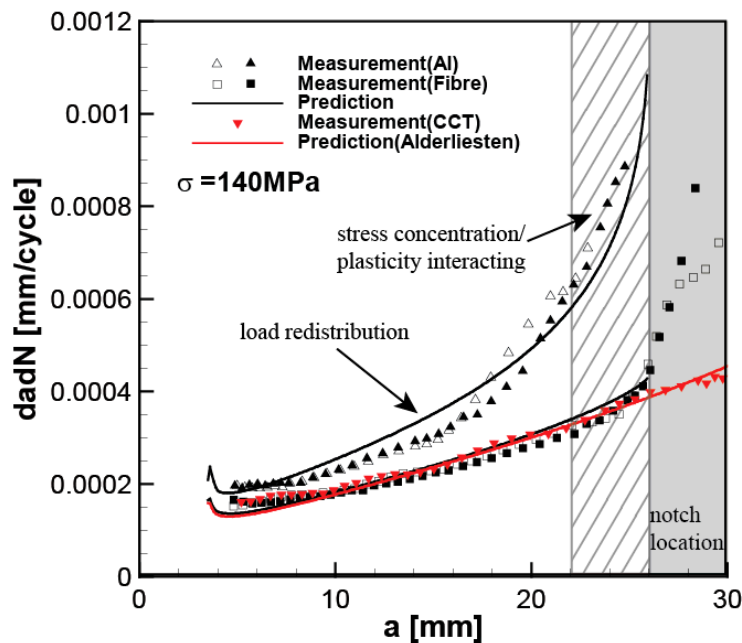


Figure 11: Comparison of effects of different stiffness reductions on the crack growth behaviour in FMLs.

3.2 Directionality of Damage Growth in Fibre Metal Laminates

Principal investigator(s): M. Gupta, R.C. Alderliesten, R. Benedictus, TUD

Fibre Metal Laminates (FMLs) were developed at Delft University of Technology in the past decades, and are currently being applied as skin material for fuselage structures. However, these days FMLs are also considered for wing applications. The difference between the fuselage and lower wing applications lies in the thickness and orthotropy of the materials, the lower wing skin

applications are primarily dimensioned for wing bending and therefore utilize unidirectional FMLs. In the past decade, the developed methodologies - refs. [14] and [15] - have described the damage growth characteristics in FMLs under static and fatigue loads without considering the direction of damage growth. However, the application of unidirectional FMLs requires the ability to describe and accurately predict the crack growth direction.

The current research investigated the crack paths of FMLs under off-axis loading. It identified the role of fibre-bridging by the off-axis fibres in deflecting the crack from its erstwhile transverse path. An analytical model was developed to predict the crack paths in different Glare grades under various off-axis angles. The results from the developed analytical model predict the trend and the values of the crack paths with reasonable accuracy. The results – both experimental and analytical – for Glare3 are presented in Figure 12. Similar agreements were observed in Glare2A, and Glare4B.

Currently, more experiments are being undertaken with larger stiffened panels. In the balanced laminate – Glare3 at 45° off-axis and in-axis Glare3 –, crack paths traverse without deflection, but in Glare3 at 67.5° off-axis laminate, crack paths deflect due to the presence of the stringer. The deflection occurs because the non-zero mixed-mode in the unbalanced laminate is affected due to the additional longitudinal stiffness. One could argue the presence of the same mechanism in balanced laminates also which is true. However, the stringer affects the mode I opening which is the denominator in the mixed-mode ratios. Therefore, the mixed-mode ratio continues to remain zero in the balanced laminate even with the presence of the stringers.

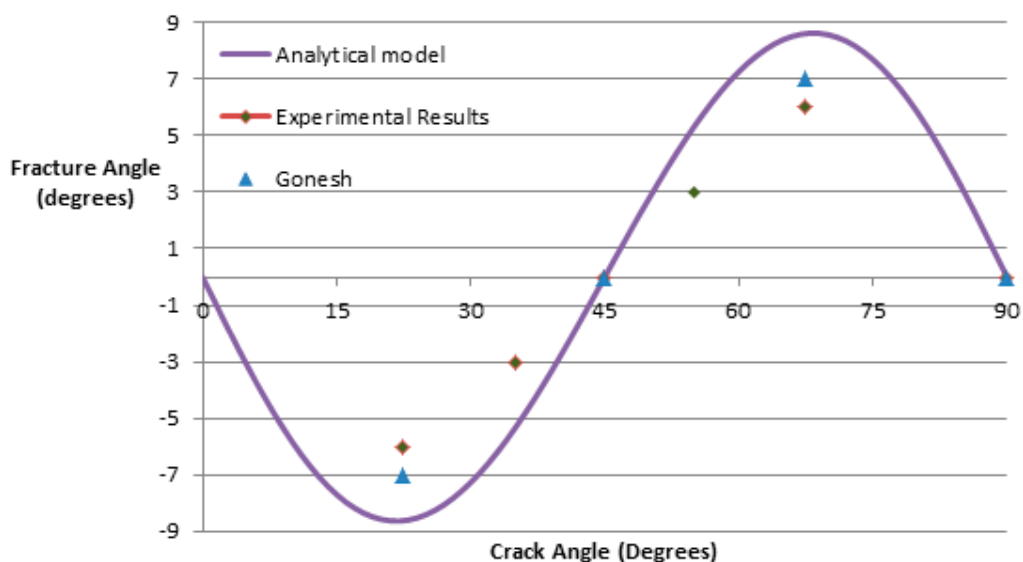


Figure 12: Comparison of experimental results (refs. [16] and [17]), and the analytical model.

3.3 Lay-up Optimisation of Fibre Metal Laminates

Principal investigator(s): I. Şen, R.C. Alderliesten, R. Benedictus, TUD

As part of a PhD project, research is performed to the optimisation of lay-ups for Fibre Metal Laminates (FML). The aim of this research is to develop a design optimisation methodology for FML to design a wing skin with a given geometry where the F&DT design criteria are met. In this method, the optimal lay-ups are obtained with the optimisation procedure by evaluating the laminates for static strength, fatigue crack initiation, fatigue crack propagation and residual strength criteria. In the literature, methods are available to predict these properties. The reversion of these prediction methods and/or the applicability of these prediction methods in a design method were extensively investigated. As a result, an optimisation procedure is developed with the use of genetic algorithms where these prediction methods for the F&DT properties are implemented as evaluation criteria.

However, the evaluation of lay-ups using the prediction methods requires a high computation time due to the many iterative calculations in the prediction methods. Therefore, a fitness approximation is considered by means of regression analysis. An approximate function is created for the prediction methods to be used in the routine, which reduced the computation time immensely, replaced the prediction method with high accuracy and resulted in the same design solutions.

The lay-up solutions are defined by three parameters: the thickness of metal layer, the number of metal layer and the grade, in which the amount and orientation of the fibre plies are defined. With the optimisation method, the lowest weight lay-up solution in the design space is determined using genetic algorithm. The algorithm generates solutions based on crossover and mutation operators and ranks the satisfying solutions based on their weight. The method is extended to consider cross-section optimisation in which only the number of metal layers is optimised along the cross-section and the thickness and grade is fixed to comply with manufacturing constraints. Furthermore, additional constraints were introduced to maintain compatibility between lay-ups on the cross-section and to reduce the number of design solutions.

Finally, the cross-section optimisation is linked to an analytical wing design model, that is now capable of dimensioning an aircraft wing structure using FML, see Figure 13 for an example output. The tool has the ability to compare and evaluate material configurations, to investigate the influence of various design criteria on the lay-up solutions and to optimise the material for the wing structure for minimised weight by considering real load cases and a parametric definition of the wing structure.

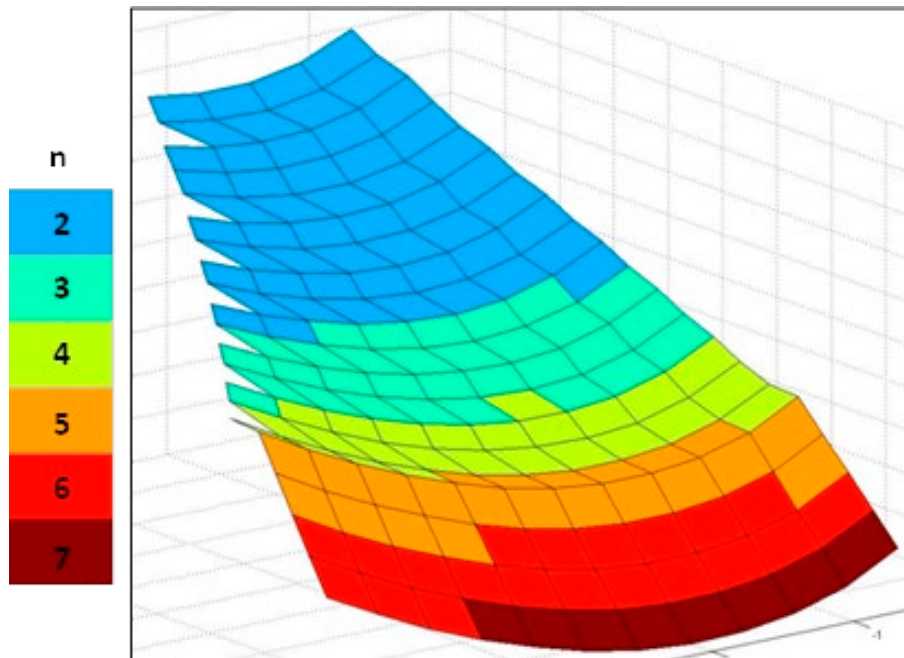


Figure 13: Wing optimisation based on $Glare2A-n/(n-1)-0.8$, n is the repetition number of a grade (number of metal layers).

4 Composite Materials & Structures

4.1 Fatigue Behaviour of Impact Damaged Thick-Walled Composites

Principal investigator(s): R.J.C. Creemers, NLR

Thick composites (>20 mm) are sometimes thought to be fairly insensitive to impacts. However, for sufficiently high impact energy levels with blunt impactors, large damages may still occur with delaminations through the entire thickness of the laminate, see Figure 14.

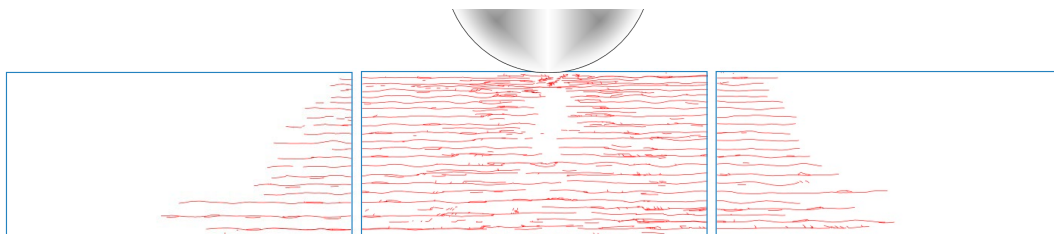


Figure 14: Slice through the centre of a specimen containing 1 inch high speed 140 J impact damage.

Static and fatigue tests have been performed on impacted laminates under compression loading. In both cases failure/damage growth is preceded by sub-laminate buckling. The damage pattern governs whether sub-laminate buckling occurs at the front or at the back of the laminate. This in turn depends on the impactor shape and energy level. Figure 15 shows that the damage grows

across the width of the specimen (perpendicular to the loading direction) and that in this particular case damage growth starts at the small delaminations at the front (impact side).

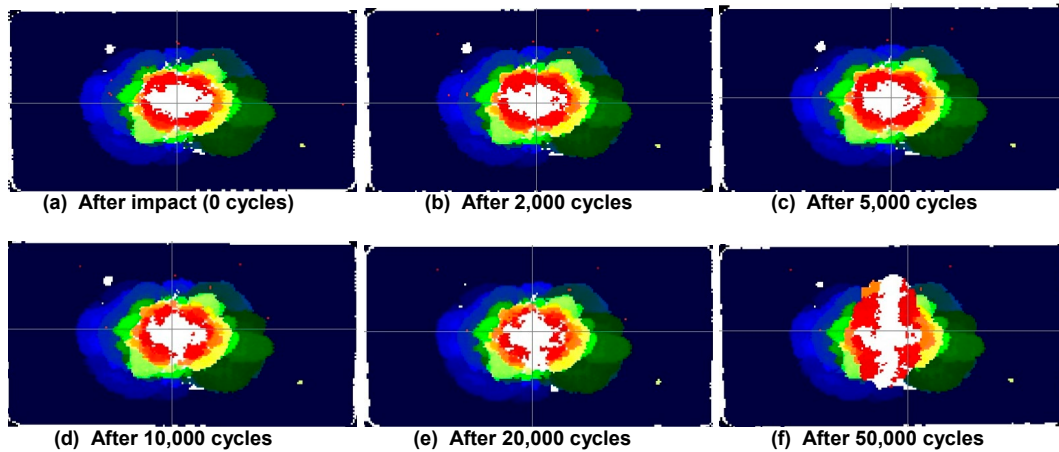


Figure 15: C-scans of impact damaged specimen (1 inch high speed 90 J) loaded in fatigue.

The C-scans also show that it is essential to make Time Of Flight pictures, because damage growth at the small delaminations would have gone undetected when only the total enclosed delamination area in an attenuation or reflection scan would have been examined. The large delaminations at the back cover the smaller delaminations at the front until the damage grows beyond the largest delamination, which happens only just before final failure.

Some of the fatigue tests were stopped immediately after the first detection of damage growth by C-scan. Slices were cut at several locations through the damaged area. This revealed a remarkable phenomenon. It became clear that damage growth was not governed by the classical mode I/mode II delamination growth. Instead, during the first phase of the fatigue test a crack had developed within the buckled sub-laminate with fibres failing in a compressive mode, see Figure 16.

During this phase no delamination growth could yet be detected. Only after this compressive crack had reached the delamination boundary, both crack and delamination would grow outwards together. The advancing delamination front is eventually detected by C-scan, but this type of delamination growth is driven by the presence of a crack in the laminate, not just by mode I/mode II delamination growth. Figure 17 gives a schematic representation of the different stages of damage growth due to fatigue.

The observed damage growth behaviour under fatigue may be only representative for the current thick specimens. However, it is conceivable that thin composites with more or less the same damage pattern (primarily delaminations and only a limited amount of fibre damage due to the impact event) will behave in the same manner. Others have performed fatigue tests on thin laminates, but to the knowledge of the authors no one has ever searched for such fibre cracks within the laminate. Usually the effort has been directed towards delamination growth and

defining models to predict such growth. However, these models can only work successfully if they address the correct failure modes. Unless experiments show that fibre cracks can be excluded from the damage growth behaviour in thin composites, it seems prudent to consider this mode for thin composites as well.

This study is reported in ref. [7].

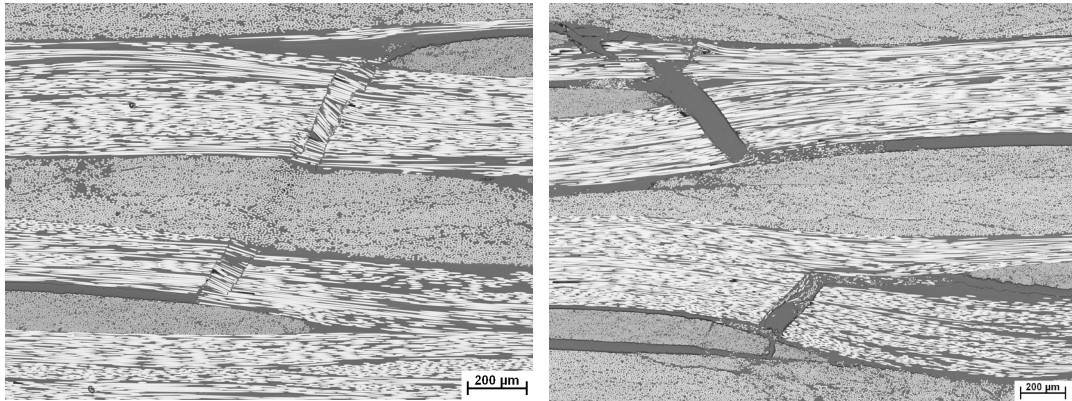


Figure 16: Left picture: kink bands at the delamination boundary. Right picture: kink bands that are pulverised under fatigue and migrate into the open delamination (deeper inside the laminate).

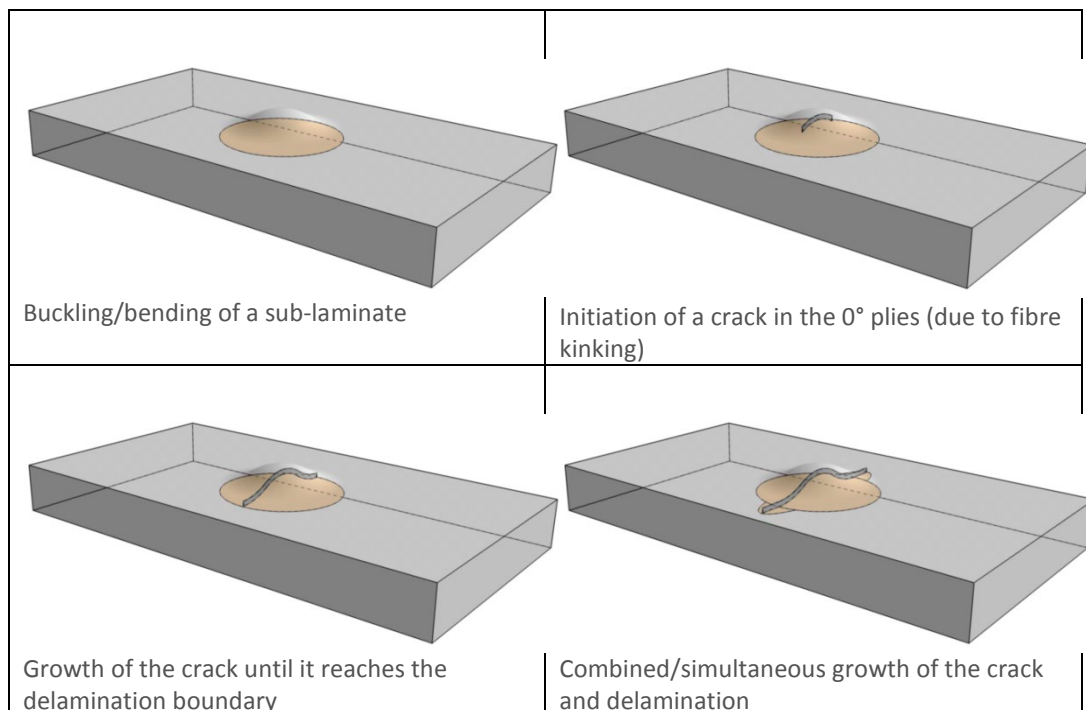


Figure 17: Schematic representation of the different stages of damage growth due to fatigue.

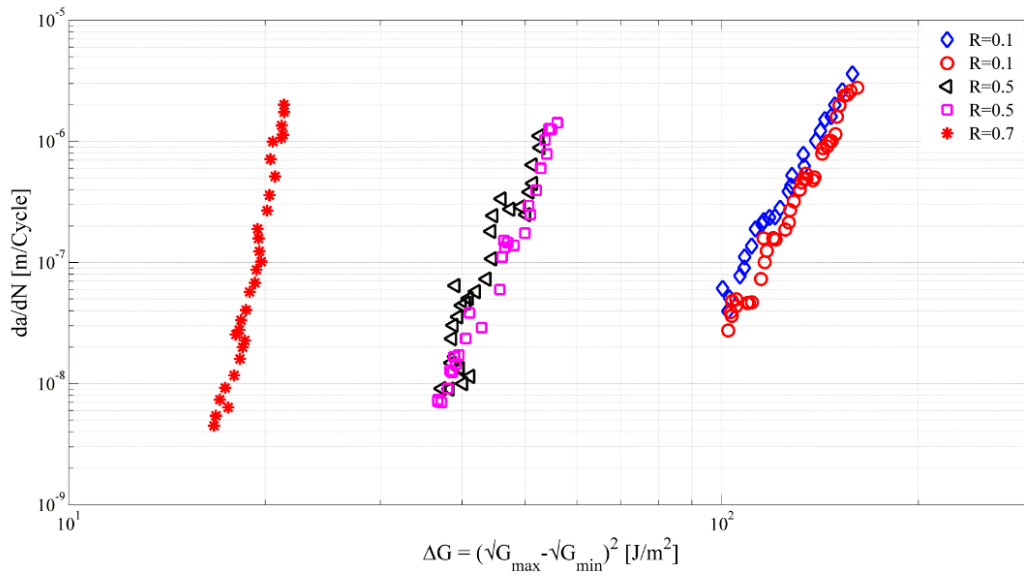
4.2 Physics based methodology for describing interlaminar ply delamination growth under mode I

Principal investigator(s): L. Yao, R.C. Alderliesten, R. Benedictus, TUD

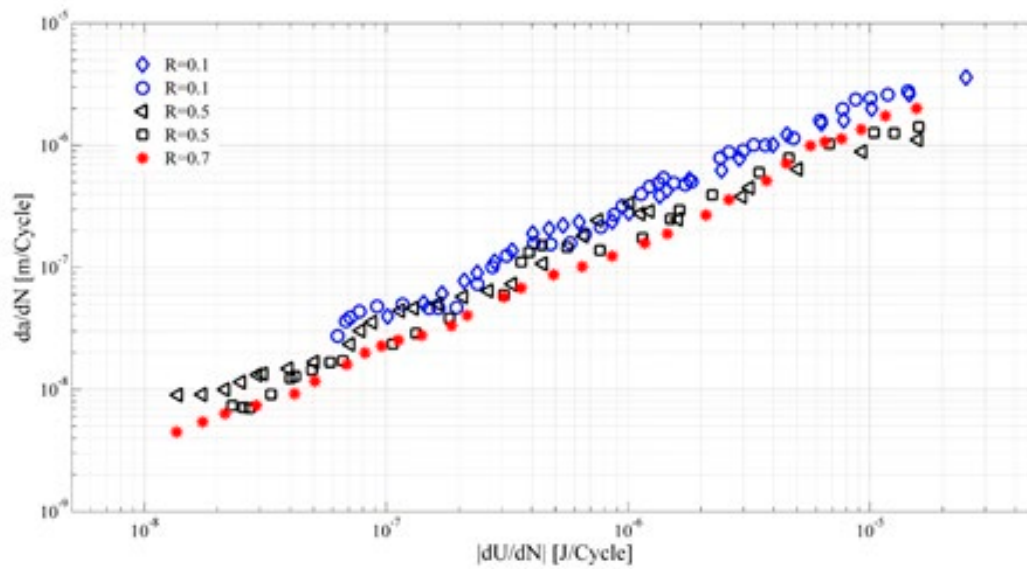
Fatigue tests were conducted on carbon fibre reinforced polymer (CFRP) double cantilever beam (DCB) specimens. Figure 18 shows the experimental data derived from fatigue tests with different stress ratios, and Figure 19 shows the data obtained from tests with different fatigue pre-crack lengths but the same stress ratio $R=0.5$. All fatigue data is interpreted with both Paris correlation and energy principle, as illustrated in Figure 18 and Figure 19.

In Figure 18(a), there is apparent R-ratio effect on the fatigue resistance curves. The R-ratio effect seems to be indistinct with the correlation between fatigue delamination growth rate da/dN and the strain energy dissipation rate dU/dN , as shown in Figure 18(b). However, taking a closer look at the results, the value of dU/dN increases slightly at the same crack growth rate with the increasing of stress ratio. This means more energy is consumed by the fatigue crack generation in a high stress ratio than that in a low stress ratio. This discovery provides an explanation with clear physical background on the R-ratio effect in fatigue crack growth.

In Figure 19(a), the resistance curves shift from left to right with the increasing of crack length. In other words, the longer the pre-crack, the lower the crack growth rate at the same value of ΔG . However, if the crack growth rate is plotted against the energy dissipation per cycle, as done in Figure 18(b) all the resistance curves converge to a narrow strip. This shows that the phenomenon illustrated in Figure 19(a) is artificial and is related to the inaccurate application and calculation of SERR during fatigue delamination analysis. Bridging fibres periodically store and release strain energy in the cyclic loading. They contribute the permanent energy dissipation only when failure occurs in them. Therefore, the actual amount of energy required to grow a crack does not depend on the amount of fibre bridging, only the stress state at the crack tip (represented by ΔG) does.

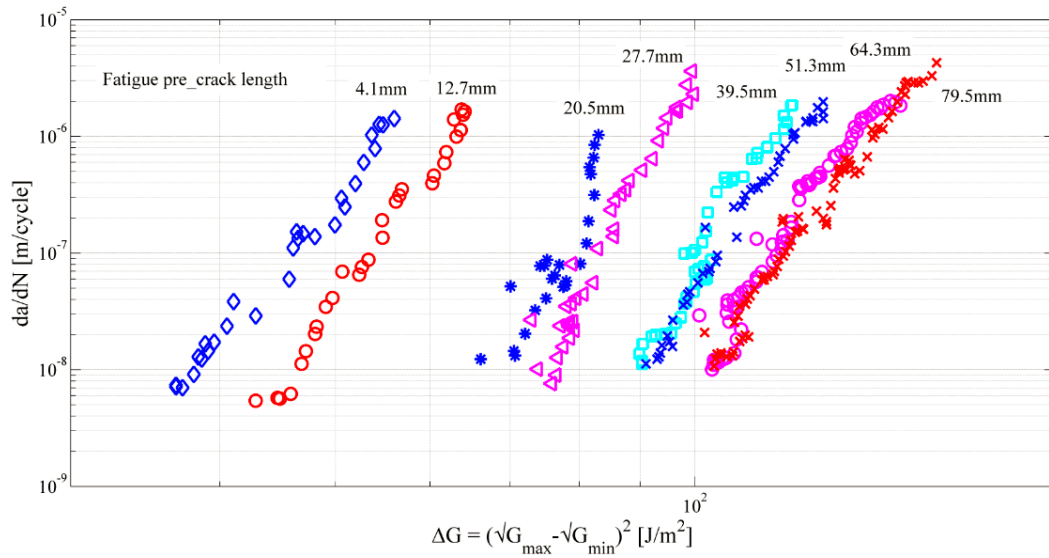


(a) Standard Paris-type correlation.

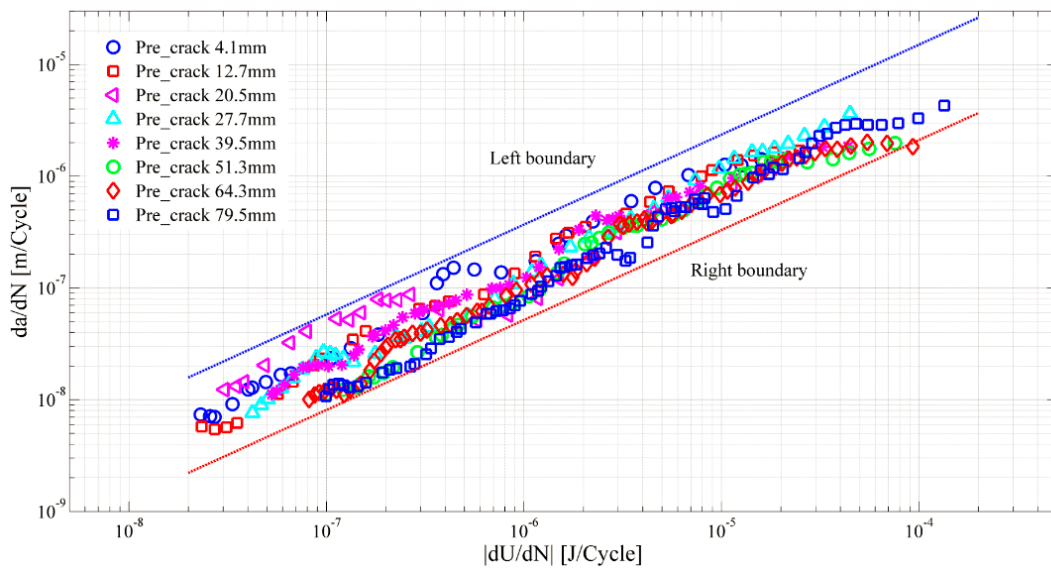


(b) da/dN against dU/dN

Figure 18: Mode I fatigue experimental results at different stress ratios.



(a) Standard Paris-type correction



(b) da/dN against dU/dN

Figure 19: Mode I fatigue experimental results with different pre-crack lengths.

4.3 Towards fundamental understanding on interlaminar ply delamination growth under mode II and mixed-mode

Principal investigator(s): L. Amaral, R.C. Alderliesten, R. Benedictus, TUD

Quasi-static data, obtained for CFRP laminated composite specimens in a mode I DCB test, can consistently be treated as low-cycle fatigue. For example, considering a quasi-static test, each drop and increase in the force can be considered a single dN , and a dU can be associated with each dN . Integrating the data in this manner and averaging the result will produce a data point in a da/dN versus dU/dN plot. However, this result is not enough to enable full understanding of the

trend of dU/da with respect to an increasing da/dN , because a single data point contains no information on the slope. In which fashion would this point move if da/dN was increased or decreased? Thus, new ways of analysing the same data with different discretization methods were necessary. Therefore, in order to analyse the trend of the data properly, the dataset was integrated in four different ways. The data was discretized to different levels, considering different number of cycles for the same crack growth.

Although each set of data is integrated with four different procedures, each set still represents the same crack extension. In other words, the fracture surface and the energy spent in creating this fracture surface quasi-statically is the same, independently of the way dU/dN was calculated. Therefore, the average values of dU/dN and da/dN were calculated with these integration procedures and plotted together. Data corresponding to five specimens were integrated in four different procedures, yielding 20 points in the da/dN versus du/dN plot. These points were plotted together, and a linear regression was used to produce the best linear fit by the minimization of the sum of the square of the error. From the slope of this fit, it is possible to obtain a real physical SERR for the quasi-static crack extension.

This concept is illustrated in Figure 20, Figure 21 and Figure 22.

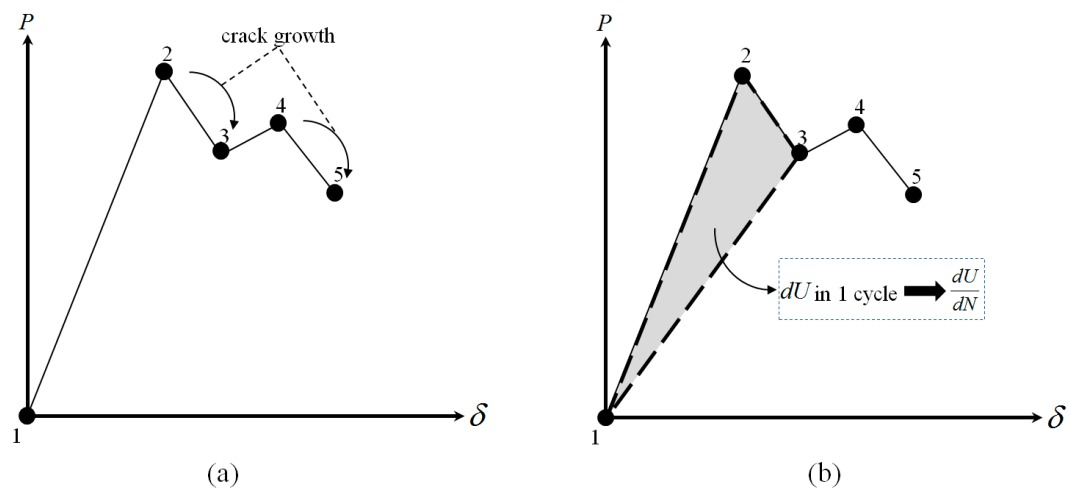


Figure 20: Illustration of the concept to discretize the quasi-static load deflection curve into low cycle fatigue cycles.

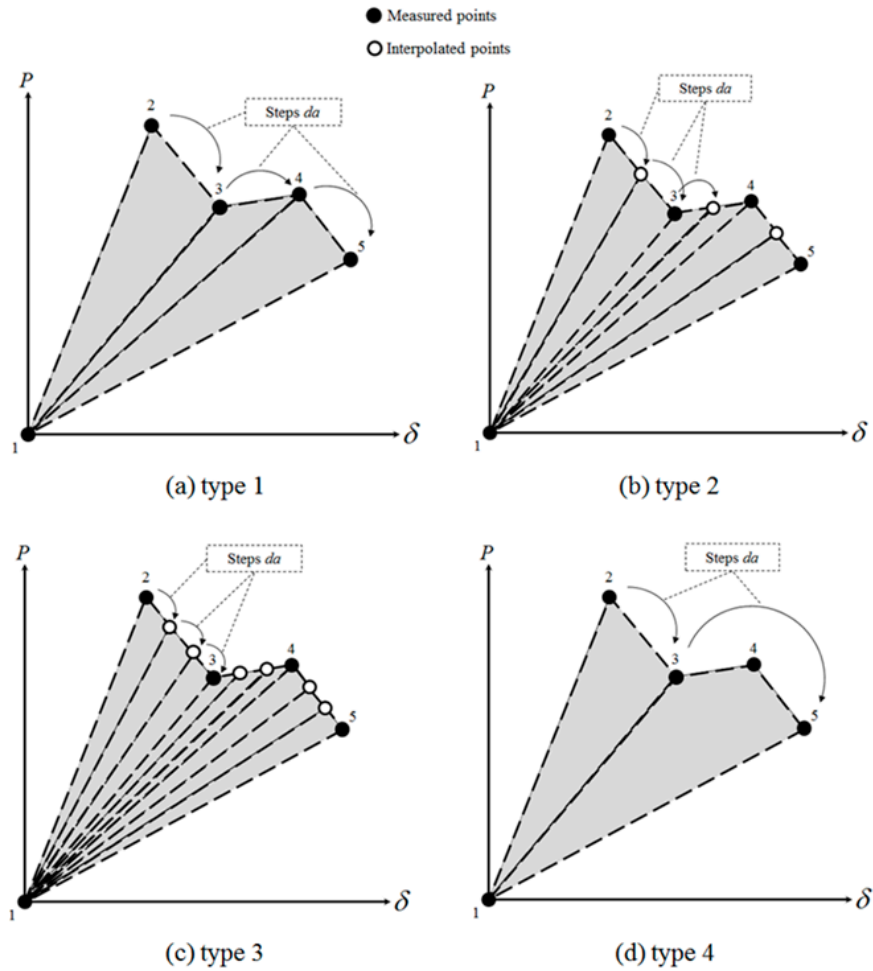


Figure 21: Illustration of the different levels of discretization of the same quasi-static data set.

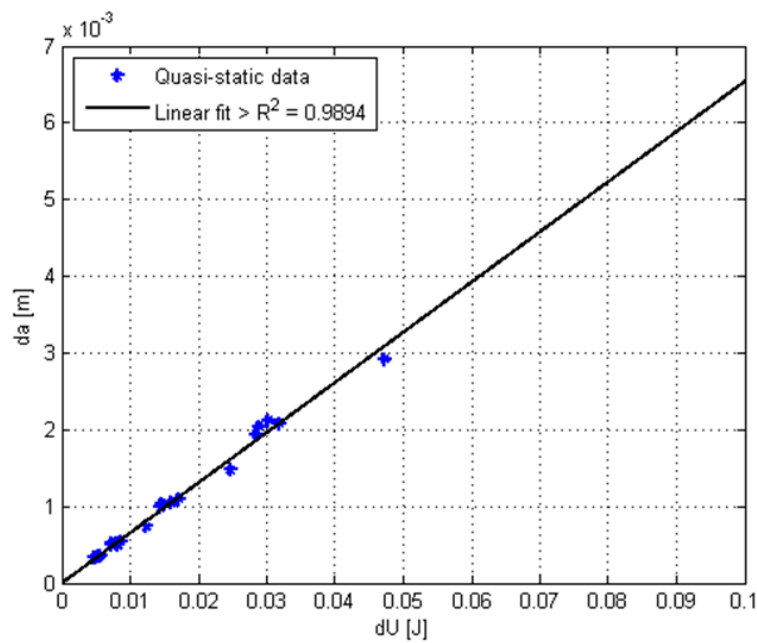


Figure 22: Average data points for different levels of discretization of the quasi-static data.

5 Adhesively Bonded Structures

5.1 Characterising the energy balance for fatigue crack growth in adhesive bonds

Principal investigator(s): J.A. Pascoe, R.C. Alderliesten, R. Benedictus, TUD

Funding: NWO Mosaic; Project Number: 017.009.005

Over the past 40 years a variety of models have been developed to predict growth of cracks in adhesive bonds, or delaminations in fibre reinforced polymer (FRP) composites. However these models are almost invariably curve fits of empirical correlations, based on modifications of the Paris relationship (itself a curve fit).

This research project aims to generate a more physics based understanding of the crack growth phenomenon by characterising the relationship between crack growth rate da/dN and the dissipation of strain energy within one cycle dU/dN , in other words, by constructing and measuring the energy balance at the scale of one cycle. The most important experimental result so far is that the R-ratio effect seen when correlating da/dN to the maximum strain energy release rate G_{max} is greatly reduced when correlating da/dN to dU/dN (see Figure 23). Furthermore, the amount of energy required to produce a unit of crack growth is not constant during a crack growth test.

For more information see refs. [11] and [12].

Data from this project is publically available from the datacentre repository of the three national Universities of Technology [13].

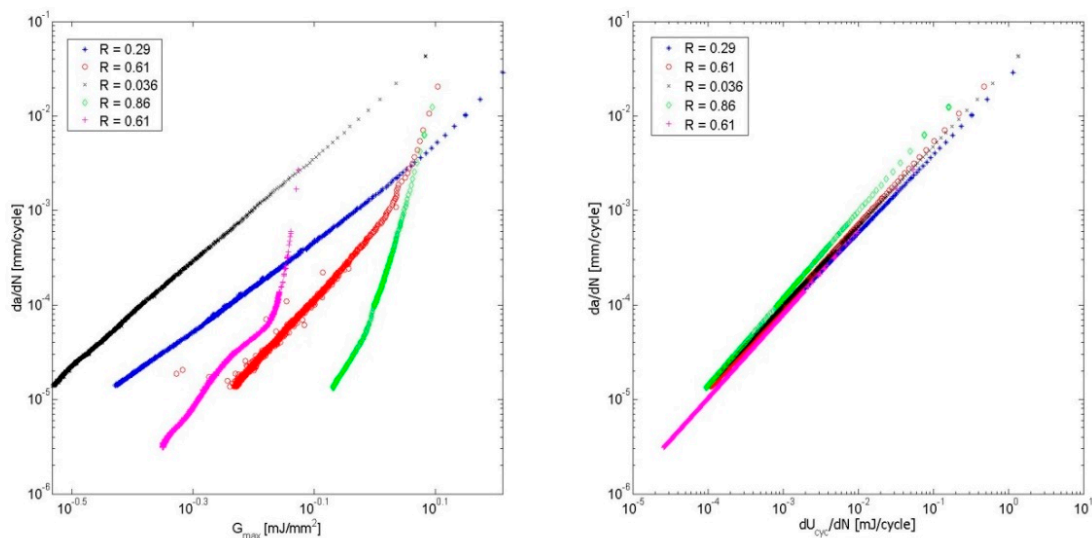


Figure 23: da/dN correlated with the maximum strain energy release rate, as is traditional (left) and with the energy dissipation per cycle (right).

5.2 Mixed-mode fatigue disbond on metallic bonded joints

Principal investigator(s): D. Bürger^{1,2}, C. Rans¹ and R. Benedictus¹

¹Delft University of Technology, Delft, The Netherlands

²Aeronautical and Space Institute, São José dos Campos, Brazil

Bonded joints can offer a more efficient load transfer than its mechanical fastened counterparts, resulting in better fatigue behaviour. However, the lack of robust fatigue and degradation prediction methods, and a lack of reliable damage inspection techniques still hinders the widespread use of bonded joints in the aerospace industry. In the last two years a model was developed and tested to predict the Mixed-Mode fatigue behaviour of metallic bonded joints. The model is based on an equivalent Mode I Strain Energy Release Rate in the principal stress direction (Eq. 1) and it also assumes the Paris relation exponent independent of the Mode Ratio.

$$\sqrt{G_{1_{eq}}} = \frac{\sqrt{G_I}}{2} + \sqrt{\frac{G_I}{4} + G_{II}} \quad (1)$$

The model was evaluated in three data sets, two produced by the authors and one from the literature. The predictions have shown a good agreement with the experimental results. Moreover, the predictions tend to be conservative in the cases the agreement was not good (Figure 24).

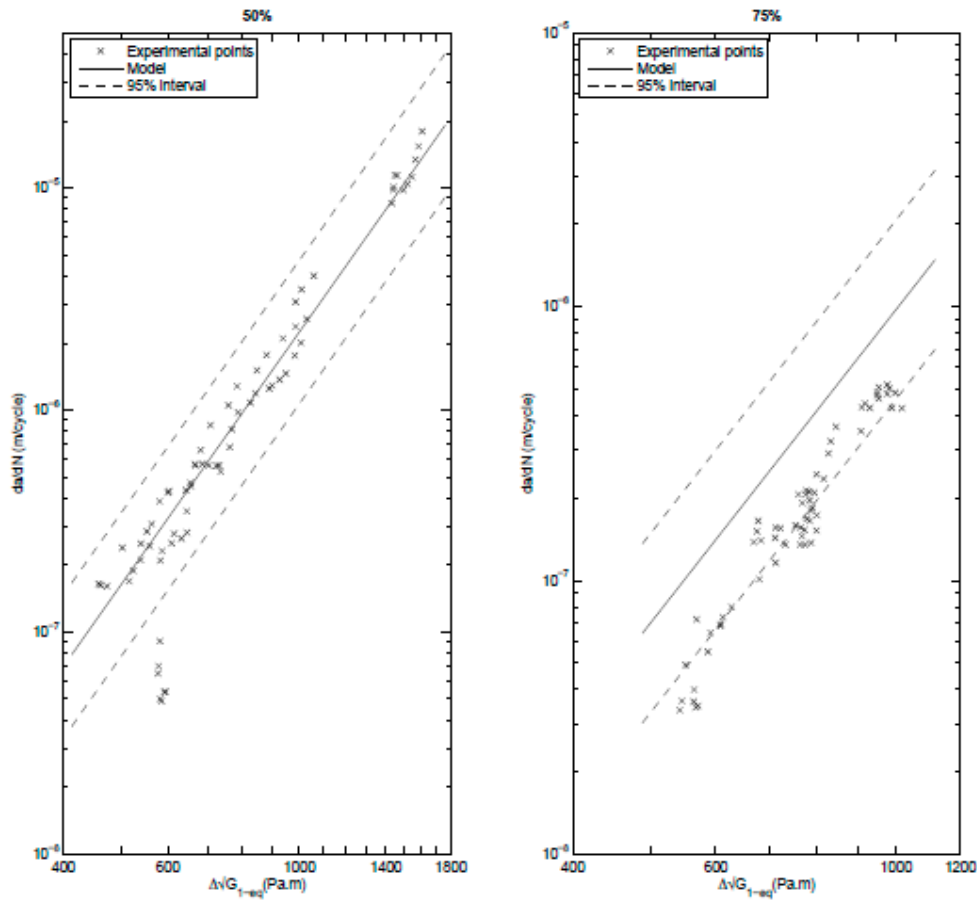


Figure 24: Model predictions for $MM = 50\%$ and 75% .

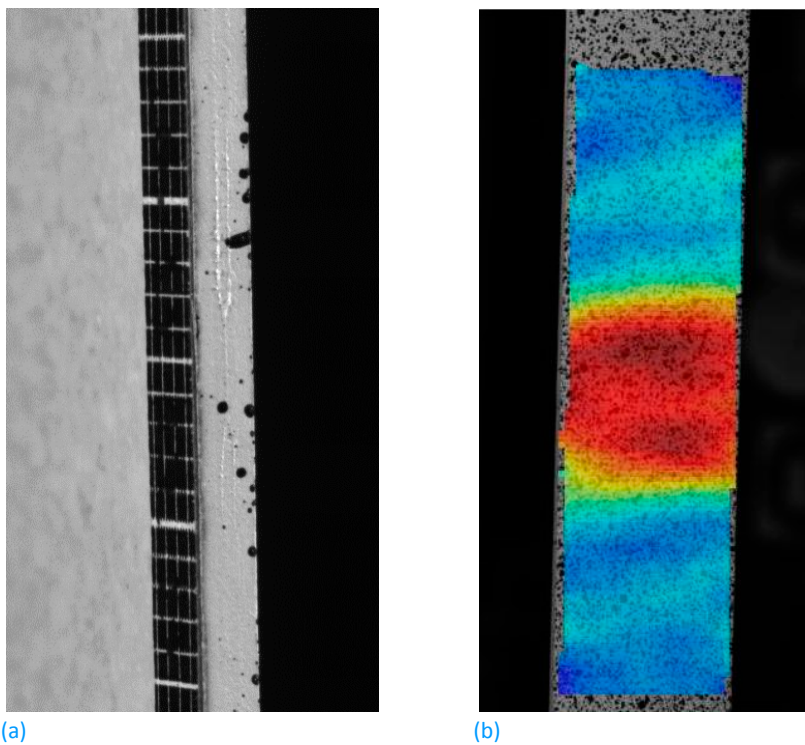
5.3 Effects of Variable Amplitude Fatigue and Temperature on the Durability of Composite Bonded Repairs

Principal investigator(s): F. Ribeiro, M. Martinez, C. Rans, TUD

Delft University of Technology is focusing on studying the effects of variable amplitude fatigue and temperature on the durability of composite bonded repairs. As part of this study, the research team aims at developing physics based nucleation model for the cohesive cracking of bonded repairs (failure within the adhesive). Since a well-designed bonded repair is expected to work mainly under shear condition, the primary focus of the research is to evaluate mode II fatigue. As such, simple variable amplitude fatigues conditions like overloads and two-level block loading will be assessed under different temperatures.

For this study, the Central Cut Ply (CCP) specimen is used for obtaining the mode II condition on the adhesive layer. Therefore, four delamination cracks can be observed on the specimen as shown in Figure 25 (a). The main advantage on the use of the CCP specimen is that the Strain Energy Release Rate (G) is independent of the crack length. This results in a constant crack growth rate for a constant amplitude fatigue loading. Therefore, variable amplitude loading

effects can be better observed from a reference (constant) value of crack growth. For the crack measurements, different NDE techniques are employed. Figure 25 (b) shows a Digital Image Correlation (DIC) analysis used for calculating crack growth from strain distribution over the specimen's surface.



(a) (b)
Figure 25: Detail of four adhesive cracks on CCP specimen (a) and DIC measurements on the specimen's surface (b).

6 Metallic Materials and Structures

6.1 Development of Physics-based principles of similitude

Principal investigator(s): R.C. Alderliesten, TUD

To describe fatigue in metallic structures and materials, different approaches are adopted. Fatigue life, or fatigue initiation life, is generally described based on stresses and stress concentration factors, whereas for crack propagation, methodologies adopting Linear Elastic Fracture Mechanics (LEFM) have been developed. Despite the differences between these two categories, they both seem to have in common that various additional corrections or factors are required. Some corrections are attributed to geometry or finite width, others to the mean stress or stress ratio, and some corrections are specifically attributed to phenomena like crack closure or plasticity.

The current study aims to better understand the physics of the problem of fatigue damage propagation in relation to the current characterisation methods. Some major findings are that the stress ratio effect generally attributed to plasticity induced crack closure, is mainly created by the way the stress cycle is characterized with using ΔK . Considering that fatigue damage growth physically is an energy dissipation process, in line with what Griffith and Irwin originally proposed, then the current methodologies are not fully adequate to for characterisation. This inadequacy is often leading to misinterpretation, illustrated by the example of plasticity induced crack closure.

Therefore, the study aims to develop proper physics-based characterisation methods to characterise fatigue damage growth resistance, in conjunction with prediction models. The study relates to similar studies in adhesively bonded structures (Pascoe et al), and composite structures (Yao et al (section 4.2), Amaral et al. (section 4.3)). In the combination of these studies a generalized physics-based theory is developed that constitutes first principles applicable to any material system, not only to metals.

For more information see refs. [9] and [10].

6.2 Improved life assessment for complex geometries

Principal investigator(s): F.P. Grooteman, NLR

The objective of this project was to improve the life prediction for complex geometries and/or complex loads by improving the accuracy of the applied stress intensity factor (SIF) solution. An overestimation of the SIF by 25% results in a factor 2 reduction in life, yielding an extensive reduction in operational life, since the SIF is raised to the power of around 3.0 in the crack growth equation. In general handbook solutions are applied in the design of aircraft components for which the SIF solution is known, for instance provided by crack growth tools like NASGRO. To apply these handbook solutions to real structures, a structural part has to be simplified in geometry and loading. By means of combining different solutions (superposition), somewhat more complicated loading conditions can be approximated, for instance the compounding method. Besides simple geometries and loading conditions, most handbook solutions are for mode I solutions under load control, i.e. a (uniform up to quadratic) remote stress is applied. There only exist a very limited number of mode II and mode III solutions and also only a few so-called displacement controlled solutions, were the applied load is a remote displacement instead of a remote stress.

SIF solutions can be computed with the aid of the finite element method. The disadvantage is that the calculation of such a solution can be very time consuming. Due to the increase in computer capacity, the better integration of computer aided design and finite element tools, and new numerical algorithms, the computation of a SIF solution today can be done much more efficient.

At NLR a lifing framework was developed with which a crack growth life analysis for a complex geometry and load can be performed much more efficient, automating the different steps as much as possible, especially the time consuming parts. The framework, schematised in Figure 26, provides a coupling of a CAD tool to define parameterised crack geometries, a finite element tool to compute the SIF solution and a crack growth tool to compute the life of the structure.

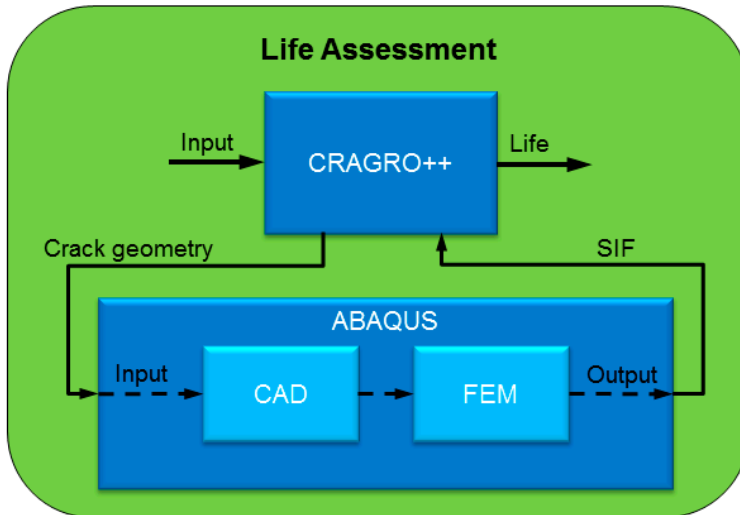


Figure 26: Life assessment framework for complex geometries and loading.

The framework was demonstrated on several one-dimensional and two-dimensional crack geometries, as well as for the F-16 wing test of section 8.1. For these examples the SIF solutions were automatically computed and, if possible, compared against handbook solutions. For a number of interesting examples, also more advanced crack growth life computations were demonstrated, e.g crack bifurcation in an integrally machined stiffened plate requiring on-the-fly SIF computation. Figure 27 shows the computed SIF and Figure 28 a deformation plot for one crack geometry showing a bifurcated crack with a crack growing simultaneous in the stiffener foot and in the web.

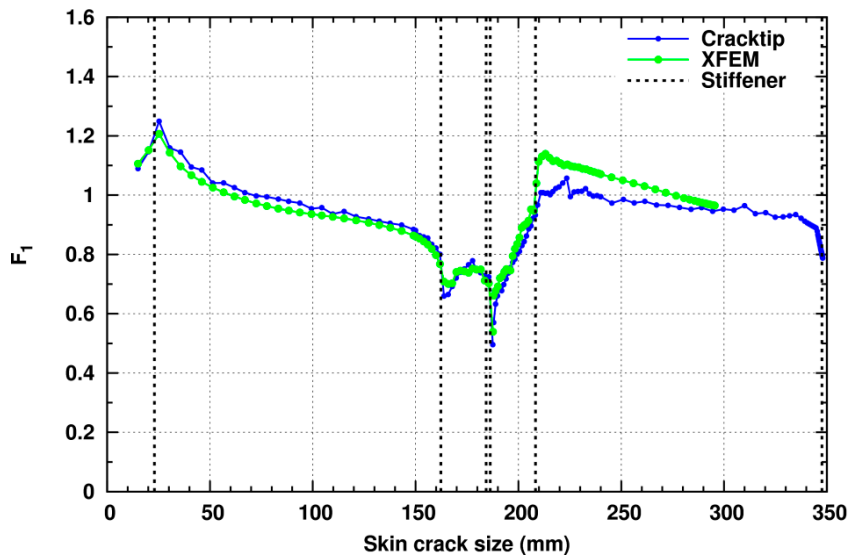


Figure 27: Obtained normalised SIF solution for the crack growth in the stiffened panel.

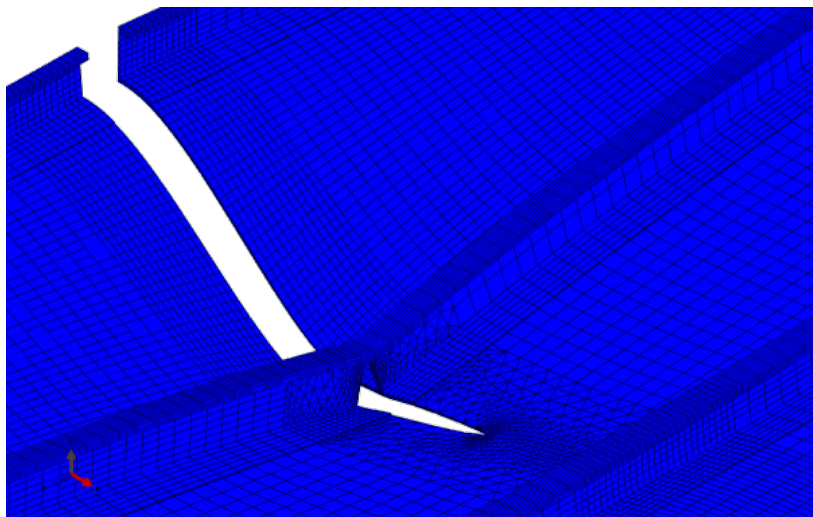


Figure 28: Deformation plot for a crack in an integrally stiffened panel.

Two different approaches were taken into account to compute the SIF solution, the conventional crack tip elements and the recently developed extended finite element method (XFEM). The conventional crack tip element approach gives the most accurate SIF solution. The XFEM approach is not as mesh independent as often suggested, but still requires a sufficiently fine structured mesh around the crack tip that correctly captures the stress field. Nevertheless, for complex geometries and/or crack shapes XFEM remains a very interesting approach.

6.3 NASGRO stress intensity solution development for a displacement controlled corner crack

Principal investigator(s): F.P. Grooteman, NLR

Many stress intensity factor solutions (SIF) exist for simple load controlled crack geometries, but only few are available for displacement controlled cases. As part of the ESA contract Structural Integrity of Pressurised Structures (SIPS), NLR computed a new SIF solution for a corner crack, schematised in Figure 29, under a displacement field.

This new stress intensity factor solution will become available within the NASGRO fracture and fatigue analysis suite extending the limited set of displacement controlled crack configurations. The displacement field consists of a complete bi-quadratic variation consisting of 9 different load terms. Two different boundary conditions were evaluated, one where the top surface is free to contract or expand in perpendicular direction and a second where the top surface is restricted in perpendicular to the load direction (fixed grip). To enable the modelling of a broad range of crack geometries in NASGRO, solutions are computed for various crack geometry parameter ranges (5 a/c ratios, 5 a/T ratios, 5 c/W ratios and 9 L/W ratios) used to interpolate a user requested solution. In total 12,600 different crack geometries were generated and analysed, requiring 53 days of CPU time on a single core of an Intel(R) Xeon(R) CPU E5-2650 processor. A few example crack configurations are depicted in Figure 30 and an example of a normalised SIF solution is provided in Figure 31.

Verification analyses were made against a few known handbook solutions.

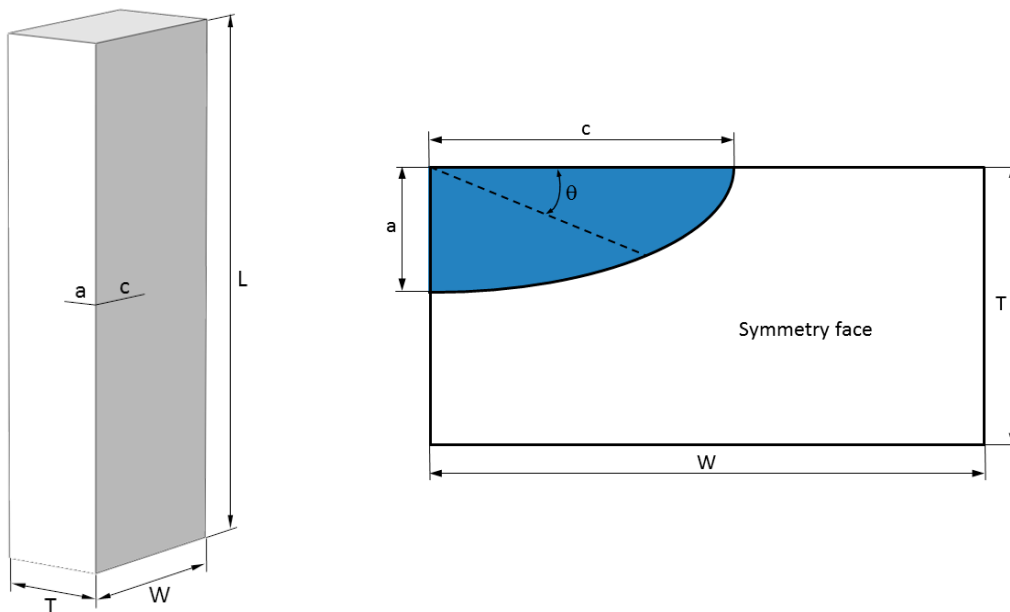


Figure 29: Schematised corner crack geometry.

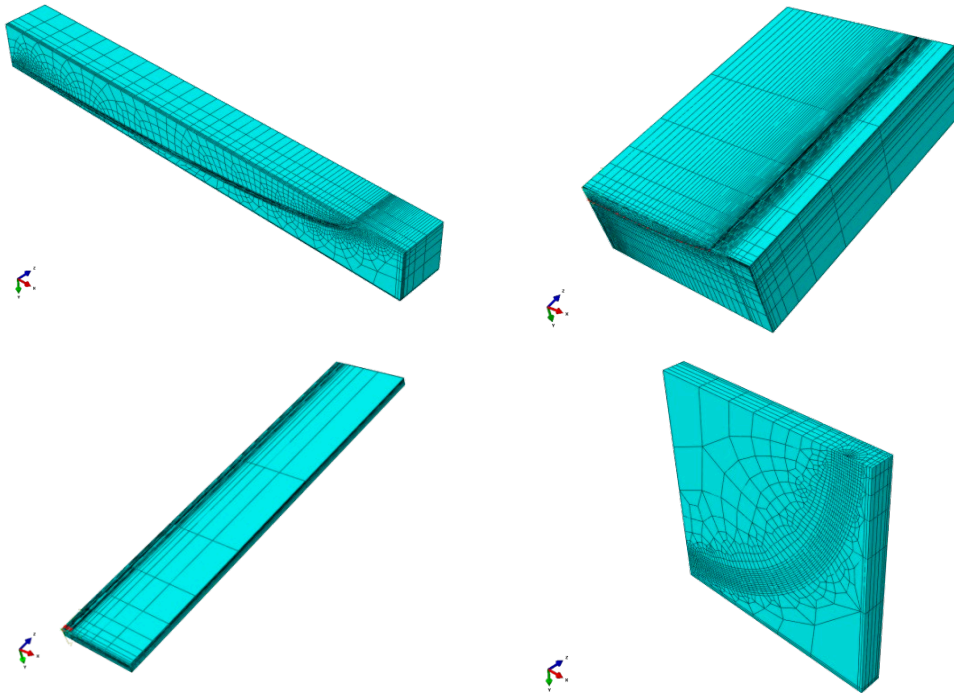


Figure 30: Examples of analysed corner crack configurations.

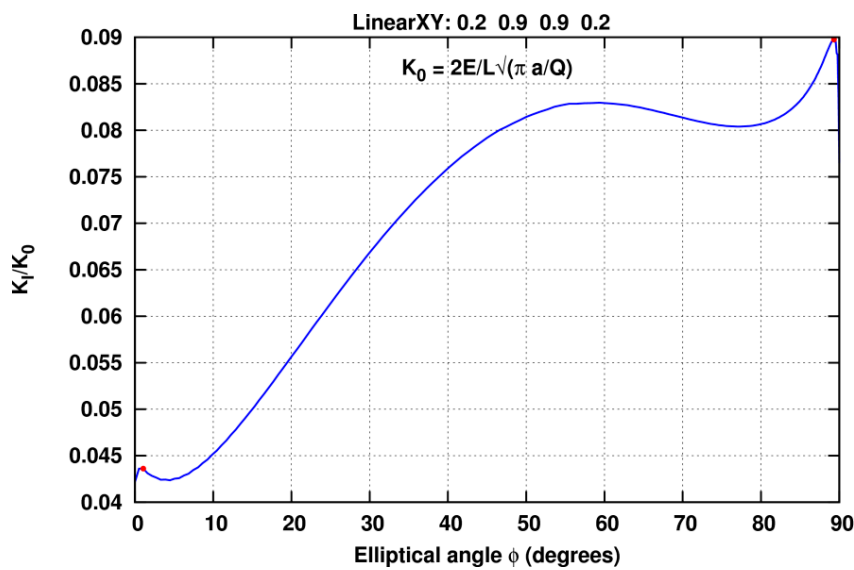


Figure 31: Example normalised SIF solution for a linear displacement field in both directions for $a/c=0.2$, $a/T=c/W=0.9$, $L/W=0.2$.

6.4 F-16 Wing Crack Severity Index evaluation

Principal investigator(s): F.P. Grooteman, NLR

For the F-16 the fatigue loads are directly monitored by means of five strain gauges for each individual aircraft – see section 2.3. To quantify the potential fatigue damage of different load spectra, the severity of the operational usage with respect to the fatigue life needs to be

assessed. For this, in the past the crack severity index (CSI) concept has been developed at NLR, expressing the severity of a load spectrum as a single value that can be easily interpreted by fleet management. Currently, only the load spectrum measured at the wing root area (FS325) is used to compute the CSI value.

A second strain gauge is located near the BL120 location on the lower wing skin. The strains/stresses obtained at BL120 significantly differ from the wing root area and are thus more representative of the load severity in this part of the wing. The main objective of the work was to examine a possible extension of the CSI concept to this second strain gauge location. A second objective was to check the CSI concept for the FS325 location for the current usage which differs from the usage during the validation of the CSI concept in 1991. To this end, a series of fatigue crack growth test on representative MT coupons were performed for different load spectra, see Figure 32, and the results were applied to validate the CSI concept for both wing strain gauge locations.

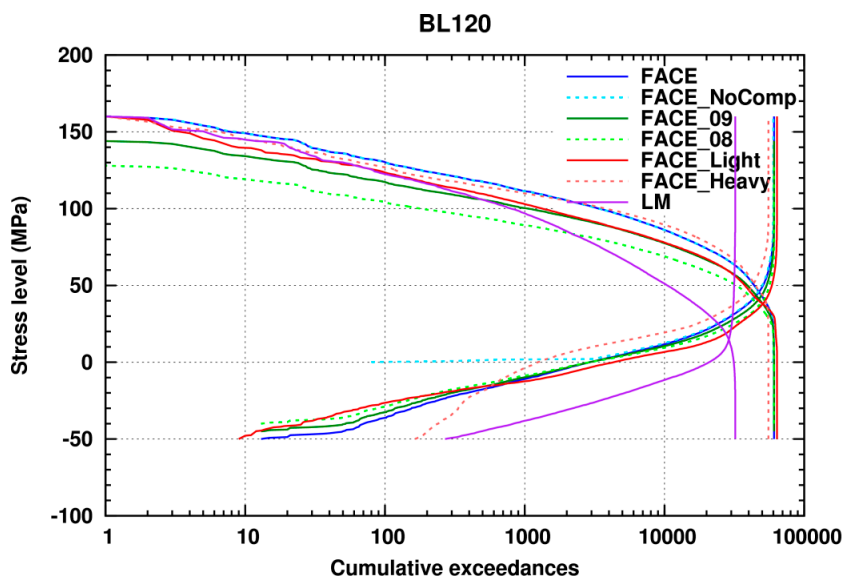


Figure 32: Stress exceedance plot of the applied BL120 test load spectra.

The obtained crack growth curves indicated that the various crack growth curves can be related to one another by a constant value, depicted in Figure 33, like the CSI. This is less the case for the, for life computation less interesting, last part of the curve. An error of (much) less than 25% was obtained for the computed CSI values compared to the experimental crack growth life ratios. It therefore could be concluded that the CSI provides a reasonable accurate measure to quantify the load severity of spectrum loads measured by both the F-16 wing root (FS325) and upper wing (BL120) strain gauges. Moreover, the experimental variable amplitude crack growth curves showed exponential growth. It was demonstrated that an approximate value for the exponential growth parameter can be derived from the CSI value.

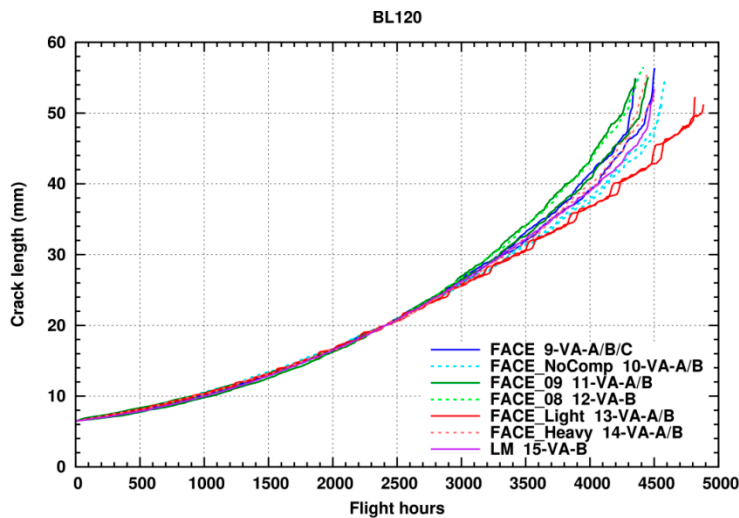


Figure 33: Scaled crack growth curves BL120 spectra.

6.5 F-16 wing test lead crack growth analyses

Principal investigator(s): F.P. Grooteman, NLR

At NLR a full-scale fatigue test campaign has been performed on a left-hand-side F-16 wing of a decommissioned F-16 Block 15. This damage enhancement test aimed to grow in-service cracks of sub-detectable size to a size where they may readily be detected. The main objective of the test was to determine if the ex-service wing contained damage not accounted for in the early durability test program that was performed in the late 1970s or in the current durability and damage tolerance analysis (DADTA) of Lockheed Martin (LM). Details are provided in section 8.1. The lead crack configuration, depicted in Figure 34, that occurred in the test consisted of a crack in the lower wing skin starting at the rectangular cut-out at Butt-Line 71 growing to the spar and finally to the pylon hard point. During this period, other relevant cracks started at nearby locations in the rectangular cut-out, pylon hard point and in the underlying spar, interacting with this crack.

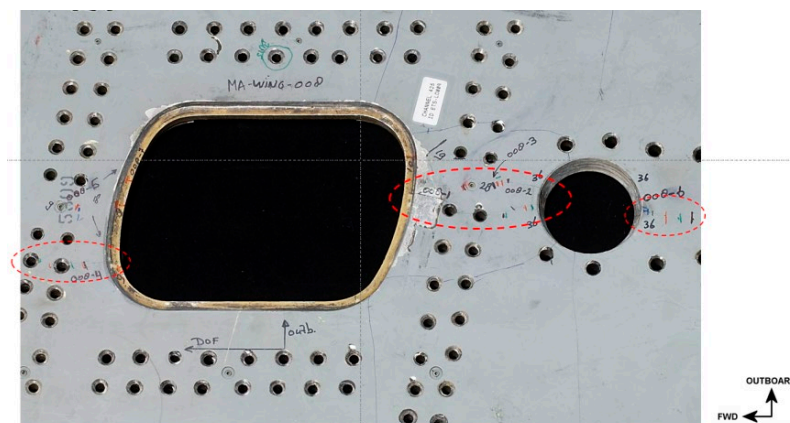


Figure 34: F-16 Block 15 Wing lower skin test lead crack configuration.

An advanced crack growth analyses was performed for this complex lead crack configuration using a lifing framework developed at NLR and compared with the experimental results to determine the life prediction capability of such an analysis. First, Mode I and II Stress Intensity Factor (SIF) solutions were computed for each of the 23 unit actuator loads using the F-16 Block 15 coarse grid finite element model of Lockheed Martin that is available at NLR. For this, the model was significantly refined in the region of the lead crack configuration around the rectangular cut-out. This yielded much more realistic SIF solutions instead of the simple handbook solutions normally applied, taking into account the correct wing structure, the realistic crack configuration and applied 23 actuator loads, including load redistribution from the skin to the spars during growth of the cracks.

These 23 Mode I and II SIF solutions together with the applied rainflow counted load sequence in the fatigue test for all 23 actuators was used as input for the crack growth analysis, using a special in-house developed crack growth tool, to predict the life of the F-16 Wing. The crack growth results were compared against the test results and the LM DADTA analysis results, see Figure 35. A very good correlation was obtained between the various results. This allows the model to be applied to other future crack locations in the wing, to arrive at more accurate life predictions for the Royal Netherlands Air Force usage.

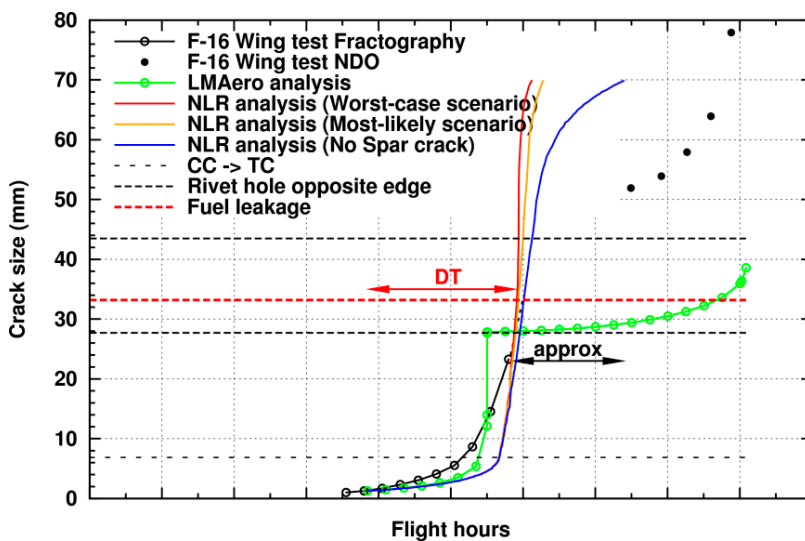


Figure 35: Crack growth life for the lower wing skin rectangular cutout lead crack.

6.6 Fatigue crack growth characterization of 3D printed Ti-6Al-4V

Principal investigator(s): L. 't Hoen-Velterop, NLR

The objective of the tests was to determine the fatigue crack growth properties of 3D printed Ti-6Al-4V material in different orientation with respect to the building direction and for two different heat treatments. To this end a total of 26 specimens were manufactured with SLM. All specimens were stress-relieve treated before removing them from the building plate. Half of the

specimens received no additional heat treatment, the other half of the specimens received a hot isostatic pressing (HIP) treatment to reduce porosity. Figure 36 shows the orientation of the specimens and the crack plane the way they were built.

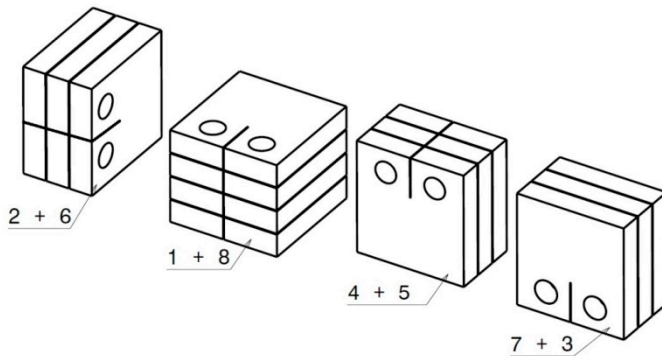


Figure 36: Building orientation of the fatigue crack growth specimens.

Constant amplitude fatigue crack growth tests were performed at a load of 3 kN and a stress ratio $R=0.1$. The crack length was monitored with the direct current potential drop (DCPD) method. An unloaded reference specimen was used to compensate for temperature differences. Optical crack length measurements were used to calibrate the DCPD measurements.

The fatigue crack growth rates thus determined showed negligible influence of the heat treatment (Figure 37). Some effect of the crack growth orientation was observed: the specimens that were in orientations 1 and 8 (green in Figure 38) showed faster crack growth while the specimens in orientations 2 and 6 (purple in Figure 38) showed somewhat slower crack growth. The microstructures of the specimens will be investigated in order to try to understand the observed differences in crack growth behavior for the different orientations.

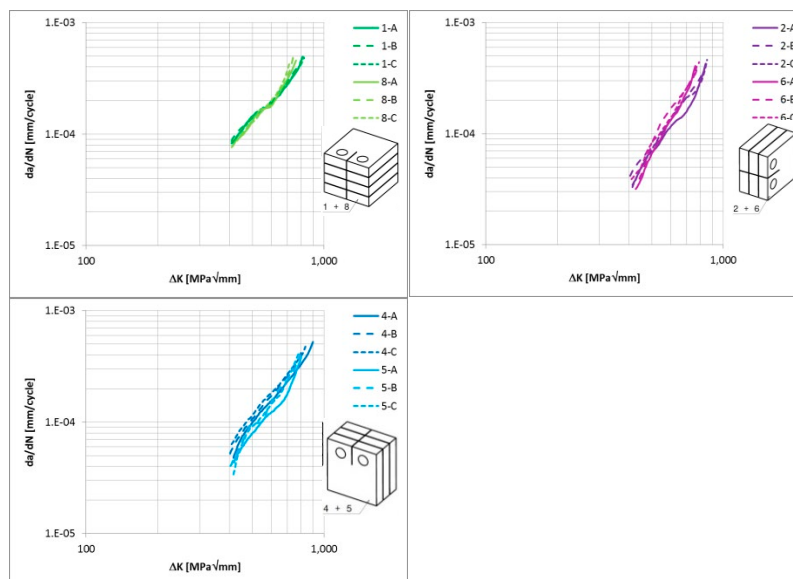


Figure 37: Fatigue crack growth rate for HIP specimens (dark lines) & stress-relieved specimens (light lines).

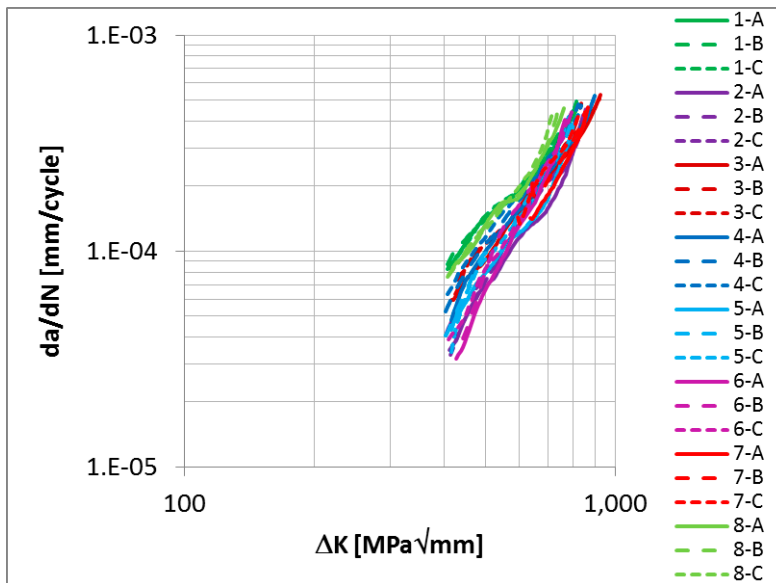


Figure 38: Fatigue crack growth rates for all specimens (specimens 1-4: HIP; specimens 5-8: stress-relieve).

6.7 The influence of stress state on the fatigue crack growth rate power law exponent

Principal investigator(s): E. Amsterdam, NLR

Paris and Erdogan [8] were the first to show that the fatigue crack growth rate in metals shows a power law relationship with the stress intensity factor range. It is generally accepted that the exponent is material-dependent. However, it is also true that the empirical Paris equation is dimensionally correct only when the dimensions of the constant in the equation are changed with the power law exponent. In the paper submitted to International Journal of Fatigue it will be shown that for 29 identical fatigue crack growth tests on aluminium alloy 7075-T7351 the exponent not only changes between materials, but also between specimens and crack lengths. Fractography and the crack length measurements show that the exponent is higher and varies at crack lengths where crack growth is dominated by plane strain conditions. The power law exponent decreases and is similar for all specimens after the transition to plane stress conditions at higher crack lengths. The mathematical concept of a pivot point will be used to model crack growth with two different exponents using a dimensionally correct equation. It also allows modelling the crack growth variation in all specimens by varying only one parameter, the power law exponent for the plane strain condition (Figure 39).

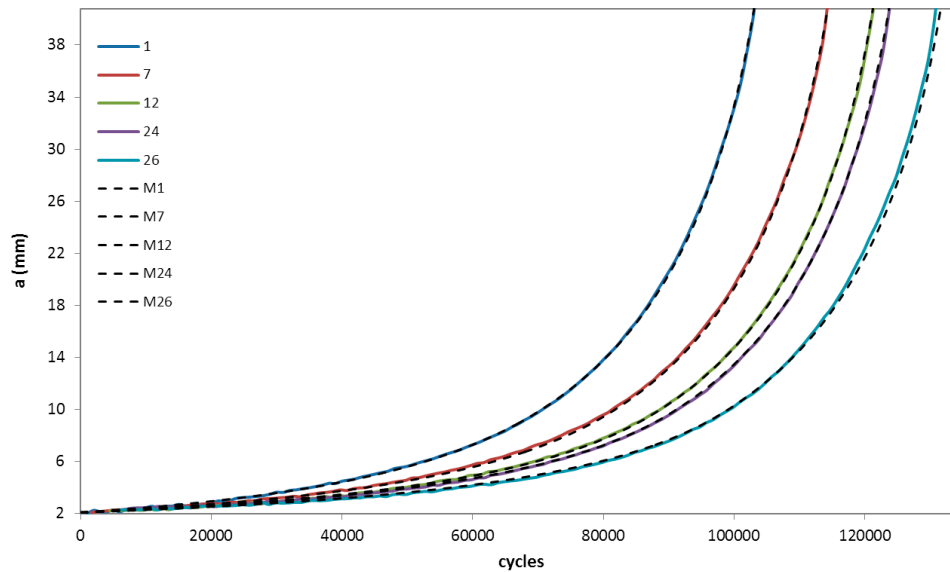


Figure 39: Crack length vs. cycles for five of the 29 specimens and the corresponding model for each specimen (dashed black lines).

7 Non-Destructive Evaluation

7.1 Air-Coupled Ultrasound

Principal investigator(s): G. Alleman¹, R.M. Groves¹, M.M.J.M. Pelt²

¹Delft University of Technology, Delft, The Netherlands

²Amsterdam University of Applied Sciences (HvA), Amsterdam, The Netherlands

Ultrasonic Lamb waves, typically generated by permanently fixed embedded or surface-mounted piezoelectric transducers (PZTs), are of interest for structural health monitoring (SHM) of aircraft. This work describes the novel combination of air-coupled ultrasound transducers (ACTs) and Lamb wave sensing using ultrasonic verification (USV). USV is an analysis procedure of monitoring the structural health of CFRP, developed jointly by the University of Amsterdam and the University of Applied Sciences, Amsterdam. ACTs overcome the problems of fixed sensor positioning and contamination by couplants by using air as a couplant. Developments in ACT technology now allow much higher energy transfer between the transducer and the structure, making the technology more accessible for aerospace applications. The objective of this research was to determine the optimum transducer parameters for damage detection. Figure 40 shows the experimental setup. A Design Of Experiments with the variables frequency, type of transducer, distance between the transducer and the material, wave mode and angle of incidence determined the parameters with the highest sensitivity to detect damage. A damage test comparing the fidelity and pulse energy methods showed that damage can be detected best with the energy method based on the variances between the measurements, difference in

percentage between undamaged and damaged signals and time windows in which damage can be detected.

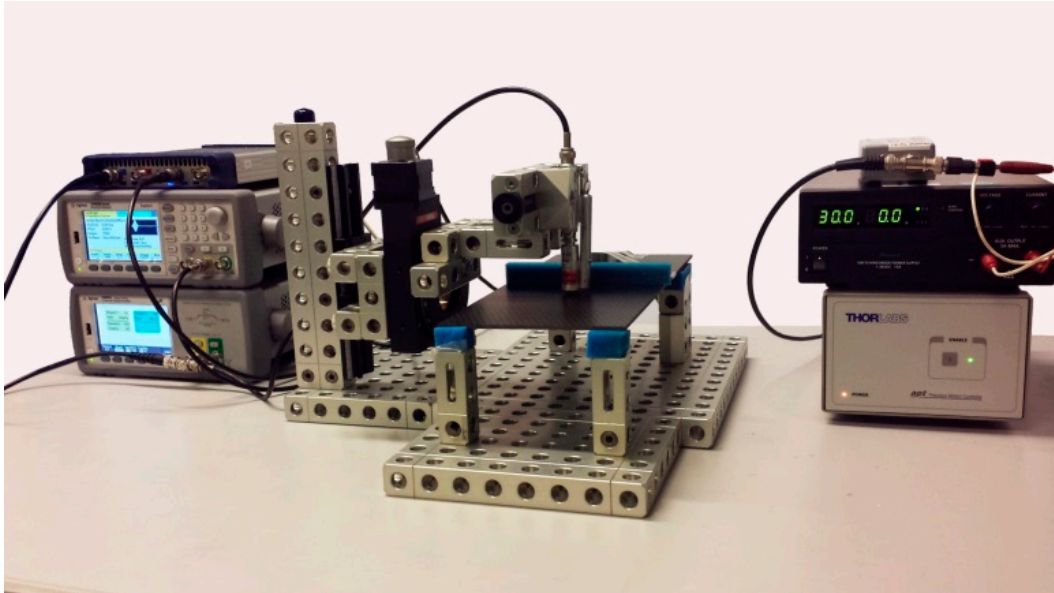


Figure 40: Experimental setup for air-coupled ultrasound.

This study is reported in ref. [18].

7.2 Detection of barely-visible impact damage in composite plates using Lamb waves

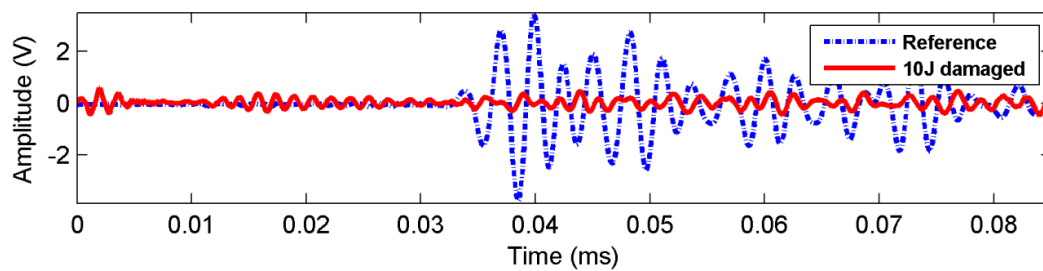
Principal investigator(s): P. Ochôa, R.M. Groves, TUD

One of the major steps of the aircraft industry towards the reduction of utilization costs and the increase of structure effectiveness has been the widespread introduction of composite materials. However, contrary to metallic materials, one of the most serious issues related to the use of composites in airframes is their brittle-type behaviour in the presence or barely-visible impact damage (BVID), which may lead to unexpected failure under fatigue loading. Therefore, the implementation of structural health monitoring (SHM) systems assumes a central role in ensuring new composite structures adhere to airworthiness regulations. Additionally, an SHM system minimizes the ground time for inspection, increases the availability and allows a reduction of the total maintenance cost.

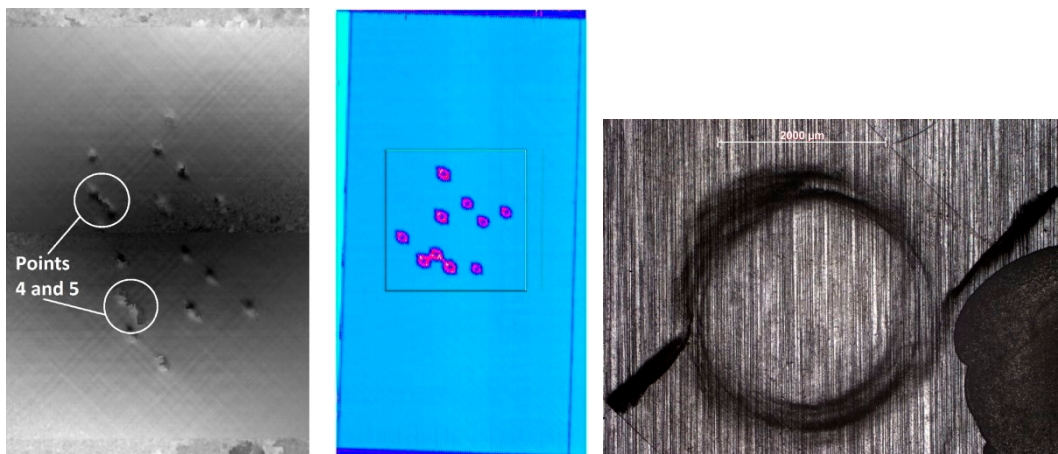
This work assesses the suitability of the two zero-order Lamb wave modes to detect multiple BVID in carbon-epoxy composite plates. Three specimens were subjected to impact damage at three different low-energy levels (3, 5 and 10 J) and one was left as an undamaged reference sample. Ultrasonic Lamb modes were selectively generated by surface-bonded piezoceramic wafer transducers in two tuned configurations. A time-domain algorithm based on the Akaike Information Criterion (AIC) was used to determine the time-of-flight (TOF) of the waves which

together with attenuation was used to define damage indexes. These proved to be sensitive enough to enable the detection of the multiple BVID on all inflicted scenarios, allowing the detailed benchmarking of the threshold detection capabilities of the fundamental Lamb wave modes for that particular application. The results were consistently validated by digital shearography with thermal loading, ultrasonic C-scan and optical microscopy (Figure 41). The study of the effects on structural integrity was completed with a global assessment of the macroscopic mechanical properties of the damaged plates. It was proven that, although the induced damage was caused by low-energy impacts, there is a considerable influence on both internal damping and static properties. In fact it was even possible to detect an effective reduction in bending strength, showing that multiple BVID may have more serious consequences during the operation of thin plate-like CFRP components than initially expected.

The first part of the study has been published in ref. [19].



a)



b)

c)

d)

Figure 41: Validation of SHM results: comparison of a) Lamb wave measurements with b) digital shearography, c) C-scan and d) optical microscopy.

7.3 Optical coherence tomography for material characterization

Principal investigator(s): P. Liu, R.M. Groves, R. Benedictus, TUD

Optical coherence tomography (OCT) is a non-invasive and high resolution volume imaging method, which allows the reconstruction of two or three dimensional depth-resolved images in turbid media. Recently Aerospace NDT Laboratory of TU Delft has developed a customized OCT instrument for non-destructive testing of aerospace materials, e.g. glass fibre composite [20]. Special attention was given to delamination growth in a 16-layer glass fibre composite [21]. The glass fibre composite was tested by incremental loading. Volumetric images obtained by OCT were further processed to reconstruct 3D crack surface profiles, from which a full field view of the delamination crack was given (Figure 42, providing substantial information for the study of crack growth in the composites. Additionally, the study explored the use of optical coherence elastography (OCE) [22] for the deformation measurement of glass fibre composites, for the first time to the best of our knowledge. The developed OCE system based on speckle tracking was implemented for a set of glass fibre composites under tensile testing and three point bending (Figure 43). The results show that OCE can measure the internal displacements of a glass fibre composite in the range from a few micrometres to hundreds of micrometres.

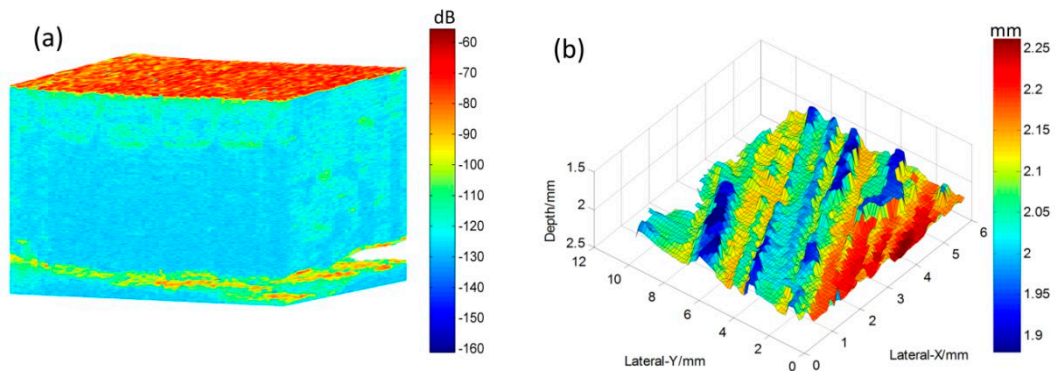


Figure 42: 3D structural image (a) of a delaminated glass fibre composite and its 3D crack surface profile (b).

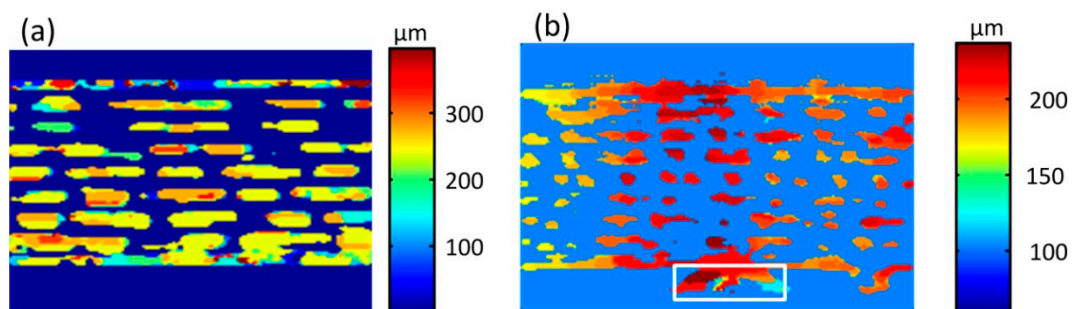


Figure 43: Internal displacement maps from a glass fibre composite under tensile loading (a) and three point bending (b).

7.4 Structural Health Monitoring based on Time_Reversal Lamb Waves

Principal investigator(s): M. Barroso-Romero, M. Martinez, R.M. Groves, TUD

Time Reversal of Lamb Waves (TRLW) is a baseline-free Structural Health Monitoring (SHM) method for damage detection that can be used on determining the health of composite structures. One primary aspect of TRLW is determining the time reversal interval required for the reconstruction of the lamb wave, necessary for further analysis and comparison with the original sent lamb wave signal. Depending on the geometry of the structure and the distribution of the SHM sensors, signal overlapping may occur between symmetric (S) and asymmetric (A) modes, and between these modes and their reflections. TUD is focusing on determining the effects of the time reversal interval on the reconstructed signal. Figure 44 shows the strategy for processing and analysis of time-reversal signals.

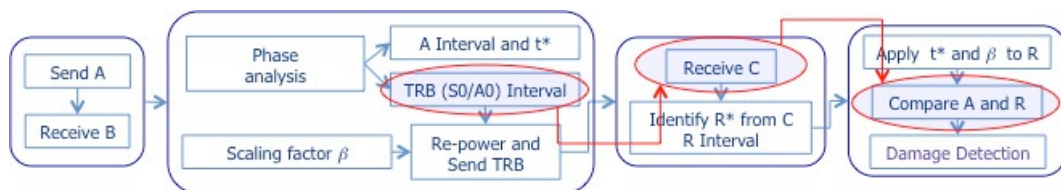


Figure 44: Time reversal process. Influence of the time reversal interval.

In our experiment depicted in Figure 45, the actuation signal A is propagated from P1 and received at P2 as response B. A time interval selected from B is time reversed to generate B*, back-propagated from P2 and received at P1 as C. The time interval for the reconstruction signal R is extracted from C. Note that the group velocity dispersion is automatically compensated in the time reversal process.

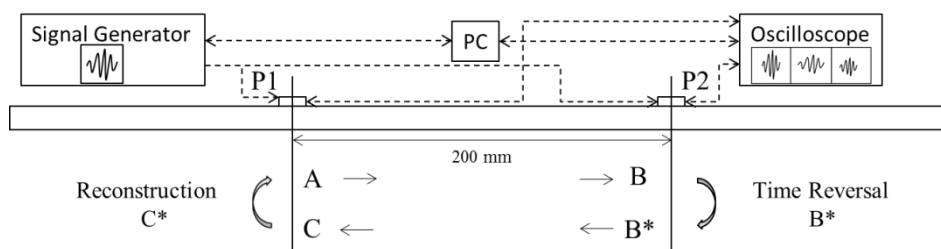


Figure 45: Experimental setup. 2 piezoelectric transducers P1 and P2 are attached to the composite laminate. A, B, B* and C are the ultrasonic signals at the transducers.

To evaluate damage, signals R and A are compared. The results show that a time interval including both modes S0 and A0 gives the best reconstruction signal R, either with and without the reflections overlapping.

This study has been reported in ref. [23].

8 Full-scale Testing

8.1 F-16 Block 15 Wing Damage Enhancement Test

Principal investigator(s): M.J. Bos, NLR

In order to verify the current estimates for the service life and maintenance requirements of the F-16 of the Royal Netherlands Air Force (RNLAf) and the Chilean Air Force (FACH), the National Aerospace Laboratory NLR in the Netherlands has conducted a so-called damage enhancement test on the left hand side wing of a decommissioned F-16 Block 15 aircraft. This durability test aimed to grow in-service fatigue cracks of sub-detectable size to a size where they could readily be detected. The main objective of the test was to determine if the ex-service wing, which had logged more than 4,000 RNLAf flight hours, contained damage not accounted for in the initial General Dynamics durability test programme of the 1970s or in the later analyses of Lockheed Martin. Other objectives were to generate data that can be used for an assessment of the current maintenance programme and to establish the most likely fail scenario. For this purpose the ex-service wing was installed in a test rig and connected to 23 hydraulic actuators which were independently controlled by means of a servo-hydraulic load control system. The rig's stiffness was designed and tuned such that the reaction forces encountered in the test rig and the internal loads in the test article closely matched the expected in-service loads for a wide range of operational flight conditions.

An impression of the test setup is provided in Figure 46.



Figure 46: Composite photograph that shows the F-16 Block 15 wing deflections as encountered during the applied limit load cases that represented -3g down bending and +9g up bending.

Prior to installation in the test rig a detailed non-destructive and visual inspection of the left hand side wing was carried out. In parallel a teardown inspection of the right hand side wing was conducted to establish the baseline damage condition. Instrumentation in the form of conventional and optical fibre strain gauges was applied for the measurement of the local strain responses in the wing skins and spars. The vertical displacements due to up and down bending were measured using a novel technique that made use of a radio transceiver mounted at a fixed point above the wing and a number of patch antennas that were bonded to the upper wing skin. After commissioning of the test setup the wing was subjected to a load spectrum representative of Netherlands operational usage. The spectrum was enhanced with marker loads to improve the 'readability' of the fatigue fracture surfaces during post-mortem fractography. Throughout the test the wing was regularly inspected for the formation and growth of fatigue damage. For this purpose standard eddy current technology was used as well as an acoustic emission system and a comparative vacuum monitoring system. Strain surveys were performed at pre-set intervals to verify the proper loading conditions.

Upon completion of the damage enhancement test the left hand side wing had been subjected to a load spectrum that was equivalent to more than twice the certified service life. During the test a number of fatigue cracks had initiated and grown, some of them to a significant size. The wing was able to sustain the three limit load cases that were applied after the durability test, however.



Figure 47: Eddy current inspection of the fatigue critical areas in the F-16 Block 15 left hand side wing during teardown.

Review of aeronautical fatigue investigations in the Netherlands during the period
March 2013 - March 2015

In the subsequent teardown analysis of the left hand side wing – see Figure 47 – the lead cracks were investigated using optical and scanning electron microscopes. Quantitative fractography, enabled by the application of marker loads in the test spectrum – see Figure 48, yielded valuable information that was used to calibrate the available fatigue crack growth models and to update the current estimates for the service life and maintenance requirements of the F-16 Block 15 wings of the Netherlands' and Chilean air forces. The inspection and test results enabled the RNLAf and the FACH to re-assess the need for their planned modification programmes and the acquisition of new wings for subsets of their fleets to ensure the required operational availability up to the phasing-out of the last F-16 in their fleets. Based on the test results and the ensuing analyses, an example of which is given in section 6.5 of this National Review, the RNLAf has decided to cancel the plans for acquiring a set of 28 new wing sets, which led to a saving of approximately 30 MEuro.

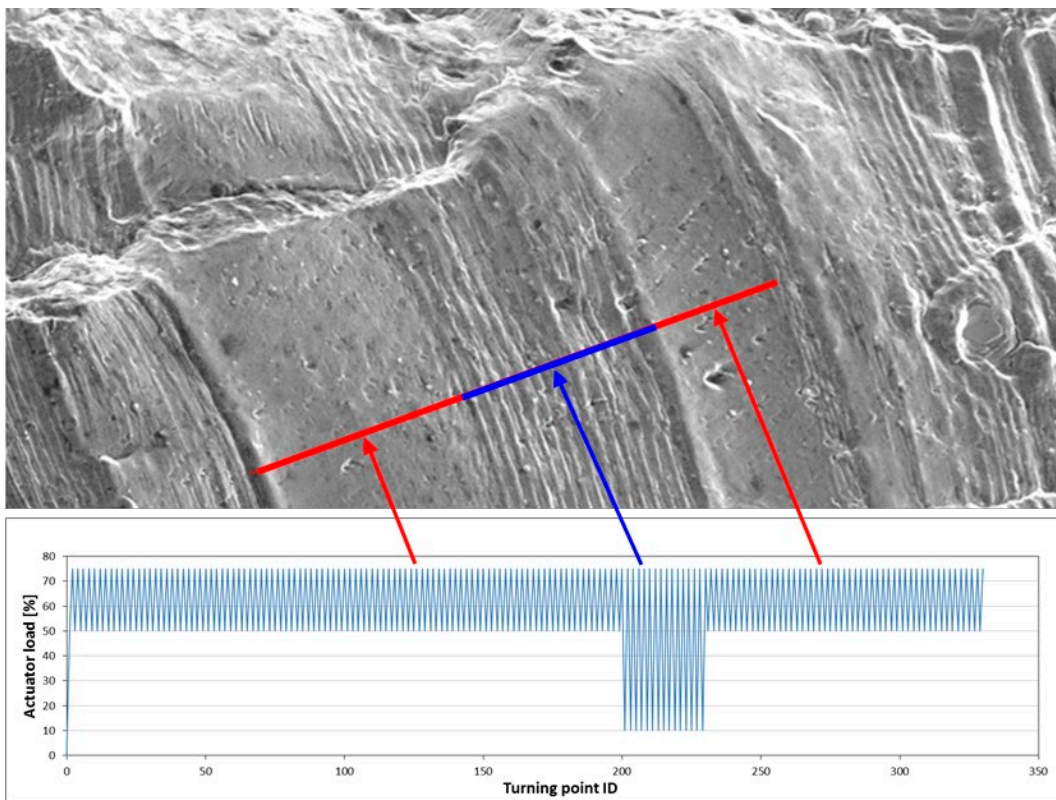


Figure 48: Fracture surface pattern for a block of marker loads.

This work has been presented at the 2014 USAF Aircraft Structural Integrity Program Conference, in San Antonio, Texas, USA – see ref. [24].

9 Special Category

9.1 Milestone Case Histories in Aircraft Structural Integrity (Update 2015)

Principal investigator(s): R.J.H. Wanhill¹, L. Molent², S.A. Barter²

¹National Aerospace Laboratory NLR, The Netherlands

²Defence Science and Technology Organisation, DSTO, Melbourne, Australia

This article/report is an update, with additional contributions, of a chapter published in Volume 1 of Elsevier's major reference work 'Comprehensive Structural Integrity' in 2003 - ref. [25] and ref. [26]. Six accidents that have especially influenced the evolution of aircraft structural integrity principles and methods are discussed. A summary includes ongoing developments in fatigue analyses and the implications of using newer materials, particularly composites, for maintaining and improving structural integrity.

10 References

1. M.J. Bos, *Review of aeronautical fatigue investigations in the Netherlands during the period March 2011 - March 2013*, NLR technical publication TP-2013-158, presented at the 33rd Conference of the International Committee on Aeronautical Fatigue and Structural Integrity, Jerusalem, Israel, 3 and 4 June 2013.
2. M.J. Bos, *Lockheed C-130H(-30) Fleet Life Management within the Royal Netherlands Air Force*, NLR technical publication TP-2012-415, presented at the ATRI symposium 2012 in Daegu, Republic of Korea, 11 September 2012.
3. A. Oldersma and M.J. Bos, *Airframe loads & usage monitoring of the CH-47D Chinook helicopter of the Royal Netherlands Air Force*, publ. in the proceedings of the 26th symposium of the International Committee on Aeronautical Fatigue, 1-3 June 2011, Montreal, Canada.
4. M.J. Bos, A. Oldersma, Lt-Kol J. Jongstra en Lt-Kol F.J.A. Verheem. *Towards Condition Based Maintenance of Aging Military Helicopters*, NATO/STO paper MP-AVT-222-05.
5. J.H. Heida and J.S. Hwang, *Monitoring of a full-scale wing fatigue test*, NLR technical publication TP-2014-261, presented at the 7th European Workshop on Structural Health Monitoring, 8-11 July 2014, Nantes, France.
6. http://doc.utwente.nl/89656/1/thesis_T_Ooijevaar.pdf, downloaded March 26, 2015.
7. R.J.C. Creemers and M.J. Smeets, *Static and Fatigue Behaviour of Impact Damaged Thick-Walled Composites*, NLR technical publication TP-2013-511, National Aerospace Laboratory NLR, Amsterdam, 2013.
8. P. Paris and F. Erdogan, *A critical analysis of crack propagation laws*, Transactions of the ASME, 1963, pp. 528-533.
9. R.C. Alderliesten, The explanation of stress ratio effect and crack opening corrections for fatigue crack growth in metallic materials, *Advanced Materials Research* Vols. 891-892, 289-294, 2014.
10. R.C. Alderliesten, How proper similitude can improve our understanding of crack closure and plasticity in fatigue, *International Journal of Fatigue*, 2015, (under review).
11. J.A. Pascoe, R.C. Alderliesten, and R. Benedictus, *On the relationship between disbond growth and the release of strain energy*, *Engineering Fracture Mechanics*, Vol. 133, pp. 1-13, 2015.
12. J.A. Pascoe, R.C. Alderliesten, and R. Benedictus, *Methods for the prediction of fatigue delamination growth – a critical review*, *Engineering Fracture Mechanics*, Vols. 112-113, 72-96, 2013.
13. <http://data.3tu.nl/repository/uuid:c43549b8-606e-4540-b75e-235b1e29f81d>
14. R. Marissen, *Fatigue crack growth in ARALL, A hybrid aluminium-aramid composite material, crack growth mechanisms and quantitative predictions of the crack growth rate*, Department of Structural Integrity. Vol. Doctor of Philosophy, Delft University of Technology, 1988.

-
15. R. Alderliesten, *Fatigue Crack Propagation and Delamination Growth in Glare*, Faculty of Aerospace Engineering. Vol. Doctor of Philosophy, Delft University of Technology, 2005.

 16. K. Gonesh, Test results and evaluation of crack propagation in off-axis Glare, Delft University of Technology, 2001.

 17. K. Gonesh, Additional test results and evaluation of crack propagation in off-axis Glare, Delft University of Technology, 2002.

 18. G. Alleman, M.M.J.M. Pelt, R.M. Groves, *Air-coupled ultrasound for damage detection in CFRP using Lamb waves and ultrasonic verification*, Proceedings of ICAST2014: 25th International Conference on Adaptive Structures and Technologies, 6-8 October, The Hague, 2014.

 19. P. Ochôa, V. Infante, J. M. Silva, and R. M. Groves, *Detection of multiple low-energy impact damage in composite plates using Lamb wave techniques*, Proceedings XIII Portuguese Conference on Fracture, PCF2012, 2-3 February 2012, Coimbra, Portugal.

 20. P. Liu, *Optical coherence tomography for material characterization*, PhD Thesis, Delft University of Technology, 2014

 21. P. Liu, R.M. Groves, R. Benedictus, 3D monitoring of delamination growth in a wind turbine blade composite using Optical Coherence Tomography, *NDT & E International*, Vol. 64, June 2014, pp. 52-58.

 22. P. Liu, R.M. Groves, R. Benedictus, *Optical coherence elastography for measuring the deformation within glass fiber composite*, *Applied Optics*, Vol. 53, No. 22, pp. 5070-5077, 2014.

 23. M. Barroso-Romero, D. Barazanchy, M. Martinez, R.M. Groves, R. Benedictus, *Time reversal of Lamb waves for damage detection in thermoplastic composites*, ICAST2013, 24th International Conference on Adaptive Structures and Technologies, Aruba, 7-9 October 2013.

 24. M.J. Bos, *F-16 Block 15 Wing Damage Enhancement Test*, Proceedings of the USAF Aircraft Structural Integrity Program Conference, San Antonio, Texas, USA, 2-4 December 2014. <http://www.meetingdata.utcd Dayton.com/agenda/asip/2014/proceedings/presentations/P7751.pdf>

 25. R.J.H. Wanhill, *Milestone Case Histories in Aircraft Structural integrity*, National Aerospace technical publication TP-2002-251, National Aerospace Laboratory NLR, October 2002.

 26. R.J.H. Wanhill, *1.04 Milestone Case Histories in Aircraft Structural integrity*, [Comprehensive Structural Integrity](#), Vol. 1: [Structural Integrity Assessment—Examples and Case Studies](#), I. Milne, R. O. Ritchie, and B. Karihaloo (eds.), Elsevier Science Ltd., 2003
-

This page is intentionally left blank.

WHAT IS NLR?

The NLR is a Dutch organisation that identifies, develops and applies high-tech knowledge in the aerospace sector. The NLR's activities are socially relevant, market-orientated, and conducted not-for-profit. In this, the NLR serves to bolster the government's innovative capabilities, while also promoting the innovative and competitive capacities of its partner companies.

The NLR, renowned for its leading expertise, professional approach and independent consultancy, is staffed by client-orientated personnel who are not only highly skilled and educated, but also continuously strive to develop and improve their competencies. The NLR moreover possesses an impressive array of high quality research facilities.



NLR – *Dedicated to innovation in aerospace*

www.nlr.nl